DEGREE PROJECT, IN MEDICAL ENGINEERING , SECOND LEVEL
STOCKHOLM, SWEDEN 2015

Biomechanical Simulations of a Flywheel Exercise Device in Microgravity

MALIN BOIJE & MARIA JÖNSSON

KTH ROYAL INSTITUTE OF TECHNOLOGY

STH

This master thesis project was performed in collaboration with
Karolinska Institutet, KI
and European Astronaut Centre, EAC
Supervisor at KI: Hans Berg

Biomechanical Simulations of a Flywheel Exercise Device in Microgravity

Biomekaniska simuleringar av resistansgivande svänghjulsbaserad träningsutrustning i tyngdlöshet

MALIN BOIJE
MARIA JÖNSSON

Master of Science Thesis in Medical Engineering
Advanced level (second cycle), 30 credits
Supervisors at KTH: Lanie Gutierrez Farewik, Mechanics &
Victor Strömbäck Alvarez
Reviewer: Patrik Sundblad
Examiner: Mats Nilsson
School of Technology and Health
TRITA-STH. EX 2015:15

Royal Institute of Technology
KTH STH
SE-141 86 Flemingsberg, Sweden
http://www.kth.se/sth

Abstract

Bone loss and muscle atrophy are two main physiological conditions affecting astronauts while being in space. In order to counteract the effects, at least two hours of aerobic and resistant countermeasure exercise is scheduled into their working day, seven days a week. Yoyo Technology AB has developed a resistance exercise device based on the flywheel principle, providing a load independent of gravity. However, there is no biomechanical research done on the efficiency of the device in microgravity, from a human movement point of view using simulation software.

The aim of this thesis was to evaluate the effects of performing a leg press on the flywheel exercise device in a microgravity environment. Simulations of performing a flywheel leg press in earth gravity, microgravity and performing a conventional squat were done. The evaluated parameters were reaction forces, joint angles, joint moments, joint powers and muscle recruitment in the lower extremities. The simulations were done using a biomechanical simulation software based on a motion capture data collection.

From the results two conclusions were proposed. Performing a flywheel leg press in microgravity environment or on earth provides at least as much peak moment as a body weighted squat performed on earth. Furthermore, performing a flywheel leg press in microgravity will induce a higher activity level among hip extensors and knee flexors compared to performing a flywheel leg press on earth.

Keywords: *FWED; Flywheel Exercise Device; Microgravity; Biomechanical Simulation; Countermeasure Exercise; Resistance Training; Motion Capture; AnyBody Modeling System; Leg Press; Squat*

Sammanfattning

Två av de största fysiologiska konsekvenserna som påverkar astronauter när de befinner sig i tyngdlöshet är osteoporos och muskelatrofi. För att motverka dessa effekter tränar astronauterna både kondition och styrka minst två timmar varje dag under sin tid i rymden. YoYo Technology AB har utvecklat en utrustning för styrketräning som bygger på svänghjulsprincipen. Tack vare detta kan ett motstånd skapas utan att vara beroende av gravitationen på jorden. Effekterna på de nedre extremiteterna efter användning av utrustningen har hittills bara studerats i miljöer med normal gravitation. Därför var det av intresse att genomföra en analys av effekten i tyngdlöshet.

Syftet med detta examensarbete var att utvärdera effekterna av en benpress utförd på en resistansgivande svänghjulsbaserad träningsutrustning i tyngdlöshet. För att uppnå detta genomfördes simuleringar av en benpress utförd på träningsutrustningen i normal gravitation samt i tyngdlöshet. Dessutom genomfördes en simulering av en konventionell benböj. Parametrarna som utvärderades var vinklar, moment och effekt i lederna hos de nedre extremiteterna. Dessutom utvärderades reaktionskrafterna samt muskelaktivering. Motion capture data insamlades för en benpress samt en konventionell benböj och simuleringarna genomfördes sedan med hjälp av ett biomekaniskt simuleringsprogram.

Efter analys av simuleringsresultat kunde två slutsatser läggas fram. Utförandet av en benpress på en svänghjulsbaserad träningsutrustning, på jorden eller i tyngdlöshet, genererar minst lika stor toppbelastning som en konventionell benböj. Dessutom innebär en benpress i tyngdlöshet större muskelaktivitet bland höftextensorerna och knäflexorerna än samma övning i normal gravitation.

Keywords: *FWED; Svänghjulsbaserad träningsutrustning; Tyngdlöshet; Biomekanisk simulering; Motverkande träning; Styrketräning; Motion Capture; AnyBody Modeling System, Benpress; Benböj*

Acknowledgement

We have reason to dedicate our special thanks to a number of people who have helped us through the process of making this thesis project valuable and respectable. Firstly we would like to thank Assoc. Prof. Hans Berg for giving us the challenging assignment which led to the final results. His great knowledge and guidance was always inspiring and gave new liveliness to our, sometimes frozen, minds.

Furthermore we have been fortunate to have several supporting supervisors contributing with their knowledge and experience. Victor Strömbäck Alvarez has showed great patience and been important in the vast process of defining the project, structuring the method and writing the report. Assoc. Prof. Lanie Gutierrez-Farewik and Erik Dijkstra have shared their invaluable knowledge in biomechanical modeling, both in the theoretical and the practical aspect.

Besides our supervisors, we would like to thank the people at the European Astronaut Centre, in particular Alexandre Frechette and the rest of the Space Medicine Office staff, for welcoming us as their colleagues during an 11 week internship. They all helped us and enthusiastically taught us about their areas of expertise. Many great experiences have come from that opportunity.

We thank Erika Franzén and David Conradsson for letting us occupy their motion lab and for contributing to the quality of the project. A special thanks to Peter Arfert for being helpful in the production of components.

Our sincere thanks goes to Patrik Sundblad for sharing his knowledge about physiology in extreme environments and providing us the contact to the European Astronaut Centre. We would also like to show our gratitude to the people who participated as test subjects.

Last but not least, we want to thank our families and friends for bearing with us in difficult times and supporting us through this master thesis project.

Contents

1 Introduction

Since 1961, when Yuri Gagarin was the first man to enter space, the knowledge and technology in the area of human space flights have evolved a great deal. In the future a journey to Mars will be realistic, in fact NASA is already planning such an exploration and hopes for it to happen already in the 2030s [1].

The extreme environment, mainly the absence of gravity during a space flight, has many effects on the human being. Some of the main effects are muscle atrophy and bone loss [2]. Due to the absence of gravity very little muscle action is needed in the every-day life. The muscle groups responsible for keeping posture at earth are barely needed at all in space and most of the work is done with the arms. Therefore, to prevent the body from degenerating, the astronauts are recommended to perform countermeasure exercise. The training, both aerobic and resistance, is scheduled for at least two hours every day, hence, it is a significantly big part of the day for an astronaut [3].

The first astronauts spending a longer time in space were not able to walk when they returned to earth, partly due to the degeneration of muscles and bones. Even nowadays the astronauts are carried just after the return in order to prevent themselves from getting an injury before they have re-adapted to earth environment [4][2].

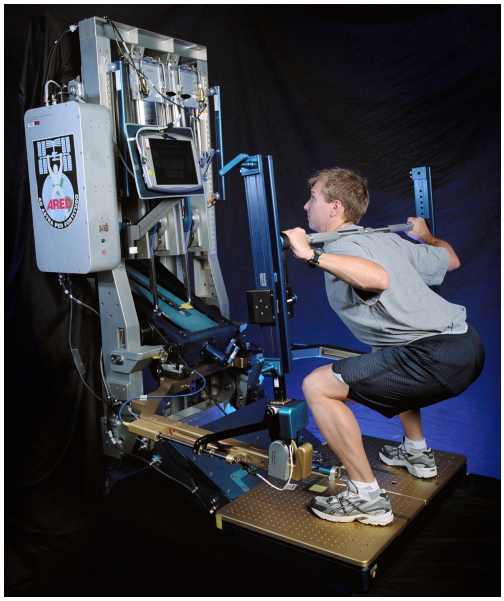

Figure 1: ARED, the exercise device used at ISS. Image courtesy to NASA.

So far the usual mission time to the International Space Station (ISS) lasts up to 6 months. A roundtrip to Mars would take at least a little longer than one year [4]. This leads to new challenges and the countermeasure exercise becomes even more important. Another aspect for a journey to Mars is the limited space. There is already an endeavor to keep weight and volume as low as possible of equipment launched to, and stored at, the ISS. This is, in addition to the limited space aspect, also due to economical reasons. Every kilogram costs around $20,000 to put into earth orbit [5].

Today at ISS, the device used by the astronauts for resistance coun-

termeasure exercise is the NASA built Advanced Resistive Exercise Device (ARED), see figure 1. The ARED is a reasonably spacious device that can provide a constant load up to circa 270 kilograms [6]. To perform aerobic exercise at the ISS the astronauts use an exercise bike or a treadmill.

In the early 90s Ass. Prof. HE Berg invented a new concept for resistive training using a flywheel [7]. Together with Ass. Prof. PA Tesch, Berg developed an exercise device using this concept referred to as a Flywheel Exercise Device (FWED). Figure 2 shows a graphic illustration of a FWED developed by YoYo Technology AB at the ISS. This type of FWED can provide the same level of peak load and has the ability to recruit the same muscle groups as the ARED, however it is a smaller and lighter device [8]. Another advantage is that the device has a relatively simple construction, which makes a potential reparation easier.

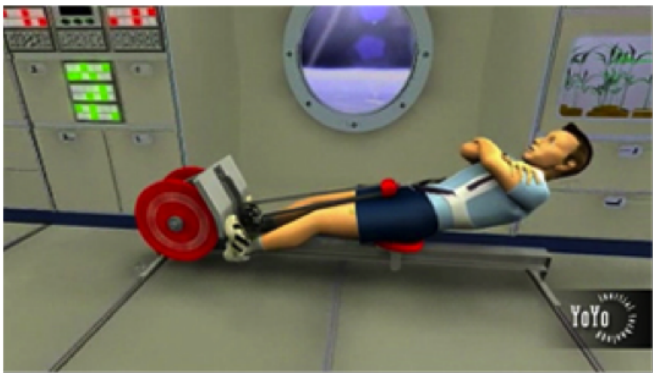

Figure 2: Illustration of the FWED at ISS. Image courtesy to YoYo Technology AB.

The FWED creates resistance through the moment of inertia produced by the flywheel. Because of this the FWED can be used in microgravity [7]. Several on earth studies have been done verifying the positive effects of the FWED when exercising the lower extremities [9][10], but almost no research has been done on the effect in orbit.

The objective of this project was to evaluate the effects of performing a leg press on the FWED in a microgravity environment. This was done by a pilot study where a musculoskeletal model was developed. The model was then used to simulate effects of exercising in microgravity. The evaluated parameters were forces, joint angles, moments and powers and also muscle recruitment. A comparison was done with the more conventional squat exercise.

2 Background

2.1 Anatomy and Physiology

In this report two motions are analyzed, a squat and a leg press. To perform this movement most of the power is produced by the lower extremities. Having this in mind, the background will primary focus on the anatomy and physiology of the lower extremities.

The body is moved by using the muscular and skeletal system, this system is called the *human musculoskeletal system*. The human musculoskeletal system gives form, support, stability, creates movement and gives protection to inner organs. The system is built up by different tissues where the basic structures are bones, tendons, ligaments and muscles [11].

2.1.1 Bone Remodeling and Bone Loss

Bone has two important functions, to serve a rigid structure needed for movement and activity, and to provide a reservoir for calcium.

Bone loss is the medical state when the bone strength is reduced due to lack of bone tissue [12]. It is known that bone loss is one of the major physical effects after being in microgravity during a long time. Data shows, see figure 3, that there is a great bone loss in the lower part of the human body of astronauts after being in microgravity for a longer period of time [2].

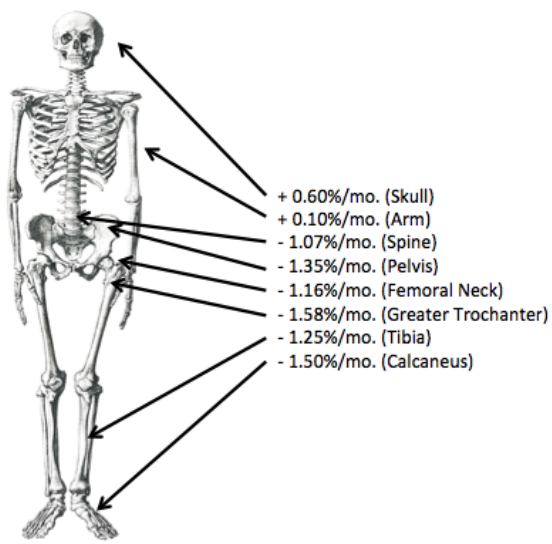

Figure 3: Compilation of bone loss rates in astronauts [2].

In 1892 Julius Wolff stated a scientific law that have formed the basis of further bone research [13]:

> "*Every change in the form and function of bone or of their function alone is followed by certain definite changes in their internal architecture, and equally definite alteration in their external conformation, in accordance with mathematical laws.*"

This law says that bone is constantly remodeled. The constant bone turnover and continual remodeling is essential for maintaining the bone strength [2].

The mechanism of sense and response due to bone loading is not fully understood. However, Harold M. Frost, introduced a model describing bone growth and bone loss called *Mechanostat* [14]. The model declares that mechanical deformation caused by load is the stimuli for bone growth or bone loss. Deformation can be shortening, stretching, twisting or bending. The deformation in length divided by the original length is called strain. Strain is usually expressed in microstrain units (μE) in the branch of biomechanics.

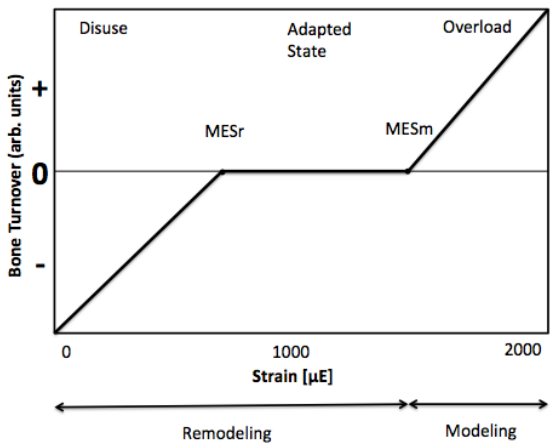

Figure 4: The bottom horizontal line shows the modeling and remodeling range. The X-axis represents strain level and the Y-axis represents bone turnover [15].

Furthermore, the model declares that the bone will adapt to the exposure of every-day mechanical loads, this will result in changes in the mechanical properties of the bone such as bone mass, bone architecture and bone strength [16].

Surrounding muscles create the largest loads on the bones, and not the body-weight as one might expect. Furthermore, the largest dynamic strains are caused by the muscles. Hence muscle strength has a major impact on affecting the architecture and strength of skeleton organs [16]. There is a linear relationship between muscle and bone Cross Sectional Area (CSA) for a healthy body [15].

A visualization of bone turnover vs. strain is shown in figure 4. There is a threshold around 800 μE for when remodeling removes bone (MESr). Consequently there is a threshold for modeling adding bone, around 1600 μE (MESm). In between these two thresholds (800 μE - 1600 μE) the bone is retained [15].

2.1.2 Joints

Joints or *articulations* are the connections between bones in the human body. The construction and function of a joint is to allow movement and give mechanical support. The surface of the bone is covered by an articular cartilage which has the ability to change its form due to mechanical loads. The articular cartilage will also protect the bones from wear. There is a small space between the bones called joint cavity filled with synovial fluid, which works as lubricant and nourishes the cartilage. The joint itself is covered by an articular capsule, which gives support and stabilizes the joint. The articular capsule is furthermore enhanced by tendons and ligaments [11].

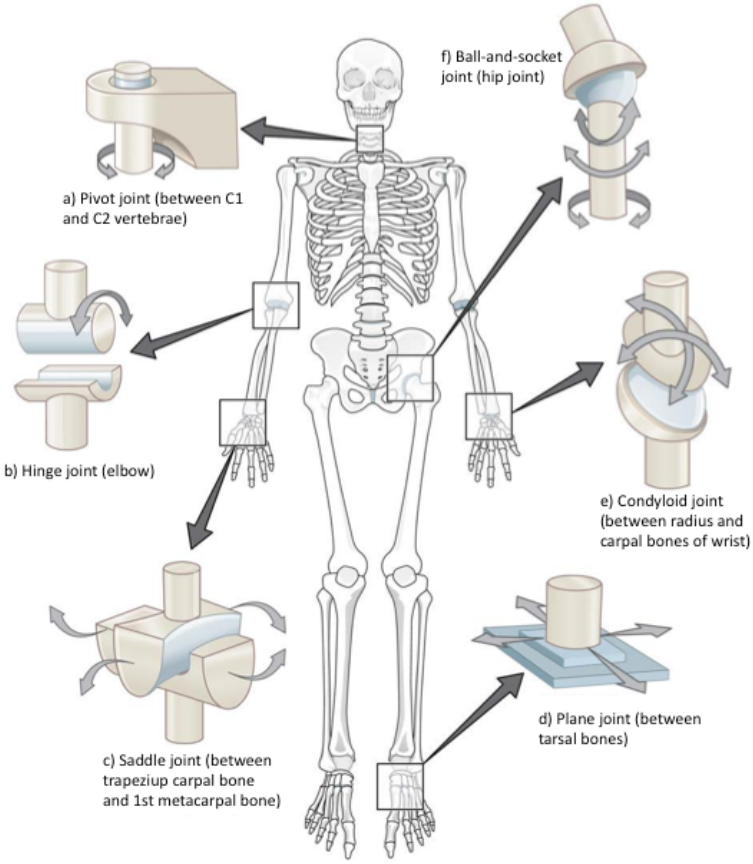

Figure 5: Illustration of 6 joints. a) Pivot joint. b) Hinge joint. c) Saddle joint. d) Plane joint. e) Condyloid joint. f) Ball-and-socket joint [17].

The classification of joints can be done by how much movement they allow. In this classification there are three different joints; *synarthroses, amphiarthroses* and *diarthroses*. The synarthroses cannot provide any move-

ment hence they are immovable joints, an example is the sutures in the skull. Amphiarthroses can provide little movement, examples are the joints between the vertebras. Diarthroses are freely moveable joints, typically the ankle and knee joints [18].

Diarthroses joints are furthermore divided into different types of freely moveable joints. These six joints are; *plane joints, condyloid joints, ball-and-socket joints, saddle joints, hinge joints* and *pivot joints* [17]. Plane joints, d) in figure 5, are nonaxial joints since they are working in one plane where two surfaces are gliding over each other. The ball-socket-joint, f) in figure 5, is working in three planes with bending and straightening in two different axes and with rotations. The hip joint is an example of a ball-socket-joint. Condyloid, e) in figure 5, works in two planes, thus it is a biaxial joint. The movements that are allowed are bending and straightening in two different axes. Saddle joint, c) in figure 5, works in the same two planes as the condyloid joint. The hinge joint, b) in figure 5, works in one plane, thus is an uniaxial joint and can perform bending and straightening in one axis. The elbow joint is an example of a hinge joint. Another uniaxial joint type is the pivot joint, a) in figure 5, the movement performed is rotational movement [11].

2.1.3 Joint Angles

The definition of joint angles in this report is based on using absolute angles (see figure 6). If the angle in the hip is positive, the hip is flexed and if the hip angle is negative, the hip is extended. In the knee joint, a negative angle is a hyperextended knee, and a positive angle is a flexed knee. In the ankle, a negative angle is a dorsiflexed ankle, and a positive is a plantarflexed ankle.

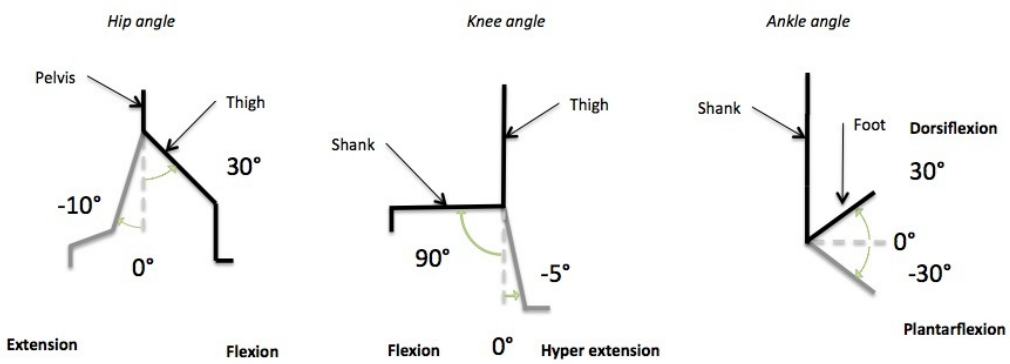

Figure 6: Illustration of joint angles in the lower extremities.

2.1.4 Joint Movements

Generally, joints are able to provide six basic movements. Two of the movements are *flexion* and *extension*, these movements can be found in the majority of diarthroses including ankle, knee and hip. Flexion is the bending movement causing the relative angle between two connected bones to decrease. The straightening of a joint, where the relative angle increases, is called extension [11]. Flexion of the hip or knee is called hip flexion and knee flexion. A flexion in the ankle joint is called dorsiflexion and extension of the ankle is called plantarflexion.

Another pair of movements is *abduction* and *adduction*. Abduction is the movement away from the midline of the body and adduction is the movement towards the midline [11]. These movements can be found in the hip joint.

The last two of the six basic movements are rotations. The rotation can either be *medial* or *lateral*. A medial rotation is when the anterior surface rotates towards the midline, where anterior is the front of the human body. Lateral rotation is the opposite, when the anterior surface rotates away from the midline[11]. This movement can be found in the hip and the knee also has a small range of rotation.

2.1.5 Muscles

There are three types of muscle cells; cardiac-, skeletal- and smooth muscle cells. The skeletal muscles are the muscles of interest regarding human movement and they serve different functions. The three functions relating to human movement are to; produce movement, provide joint stability and keep posture and positions [11].

Muscles can be classified by the joint movements they generate. If a muscle contributes to flexion in the knee joint it can be termed a knee flexor, and muscles that contribute to hip flexion or dorsiflexion are termed hip flexors or dorsiflexors respectively. Consequently, muscles can be termed hip extensors, knee extensors or plantarflexors if they contribute to hip extension, knee extension or plantarflexion respectively.

A muscle can have different fiber arrangements, the two most common fiber arrangements are *parallel* and *pennate* [11]. In a parallel muscles the fiber bundles are parallel to the muscle force direction. In the other form, penniform fiber arrangement, the fibers are arranged diagonally to the force direction.

In the parallel muscles the force works in the same direction as the musculature, hence the range of shortening is greater and a greater movement velocity occurs. The Cross Sectional Area (CSA) of a parallel muscle is rela-

tively small compared to the CSA in a penniform muscle. In the penniform muscle, the muscle fibers are shorter and work diagonally with the muscle axis, which results in a slower movement. The tradeoff is that a penniform muscle has a greater CSA and can generally produce more force [11].

There are two different fiber types, *type-I* (slow-twitch fibers) and *type-II* (fast-twitch fibers). Type-II is furthermore divided into types IIa and IIb. All types have different muscle metabolisms and energy consumptions, hence different properties. Type-I fibers, commonly known as red muscle fibers, contract slowly and are suitable for low intensity and prolonged work. Many endurance athletes have a high quantity of type I fibers. Type-IIa is also a red muscle fiber, called intermediate fast twitch fiber. This fiber type provides activity for longer periods and simultaneously provides contraction with a burst of force before it fatigues. Type-IIb, known as the white fibers, produces force quickly and then fatigues rapidly after. Many sprinter and jumper athletes generally have a greater concentration of type-II fibers. Most of the muscles consist of all types of fibers, but with different compositions [11].

2.1.6 Muscle Action

A muscle only has the capability of pulling and not of pushing, therefore it is necessary to have at least one muscle on each side of a joint to create opposing movements. Muscles generating the same joint movement are termed *agonists* and muscles generating the opposite joint movement are termed *antagonists*. When agonists and antagonists of a joint contract simultaneously, the muscles are said to be *co-contracting* [11].

When a muscle crosses over one joint, it is termed uniarticular, when a muscle crosses over two joints, it is termed biarticular. Biarticular muscles will create movements in both of the two joints crossed, but they are often more dominant in one of the two joints.

Muscle tension is generated to create a movement, control a movement or to maintain a position. When a muscle is activated but no visible change in position is shown, the muscle activation is termed *isometric*. While standing still many muscles work isometrically to hold the position and counteract gravity [11]. An isometric muscle action produces zero power.

When a muscle is actively generating tension and at the same time visibly shortens, the muscle action is termed *concentric*. In a concentric muscle action, the net muscle force is producing a movement in the same direction as the change in joint angle. In this case, the agonist is controlling the movement. Concentric muscle action gives positive power, i.e. generates power [11].

When an external moment is greater than the produced internal moment and the muscle is lengthening, the muscle action is termed *eccentric*. The net muscular force producing the movement is in the opposite direction as the change in joint angle. An eccentric muscle action gives negative power, i.e. absorbs power [11].

2.1.7 Major Lower Extremities Muscles

The lower extremities consist of muscles performing joint movements in the ankle, knee and hip joints. The strongest movement in the ankle is plantarflexion, due to larger muscle mass in the plantarflexor muscle group compared to the dorsiflexor muscles group.

Two plantarflexor muscles are the *gastrocnemius* and the *soleus*, which can be seen in figure 7 where soleus is located beneath gastrocnemius. These two muscles produce the majority of the plantarflexion force. Gastrocnemius is a biarticular muscle crossing the ankle and the knee joint, thus it is also a knee flexor. Gastrocnemius is more effective as a plantarflexor if the knee is extended [11].

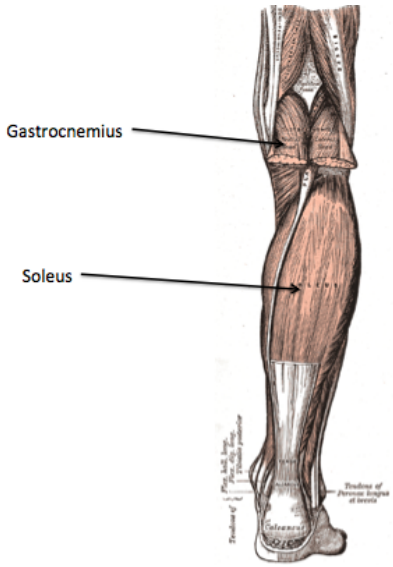

Figure 7: Illustration of the plantarflexors [19].

Knee flexor muscles and knee extensor muscles are the two muscle groups that drive the knee movement. Knee extensors have a higher force generation capacity and is therefore the stronger muscle group. The *quadriceps femoris muscle group*, consisting of *rectus femoris*, *vastus intermedius*, *vastus lateralis* and *vastus medialis* (see figure 8), is one of the strongest muscle groups in the whole body. Compared to its antagonists, the *hamstring muscle group* consisting of *biceps femoris long head*, *semimembranosus medialis* and *semitendinosus* (see figure 9), the quadriceps femoris muscle group can produce up to three times more force. The hamstring muscle group is the largest knee flexion force producer. The strongest of the quadriceps muscles is vastus lateralis. Rectus femoris is a biarticular muscle and works both as a hip flexor and a knee extensor, but is limited as a knee extensor if the hip is flexed. All hamstring muscles also work as hip extensors [11].

Hip extensor muscles and hip flexor muscles are two muscle groups that perform flexion and extension of the hip. The hamstring muscle group to-

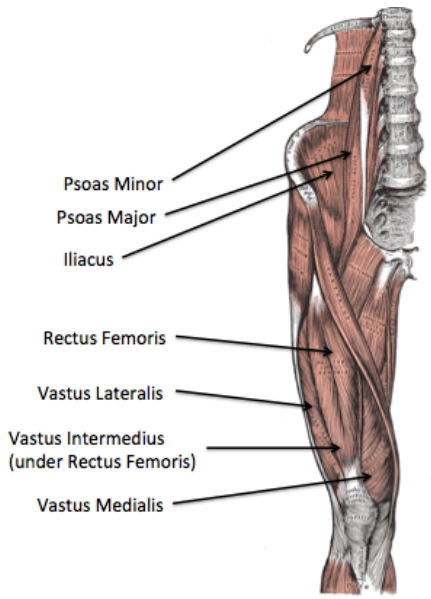

Figure 8: Illustration of the hip flexors and knee extensors [19].

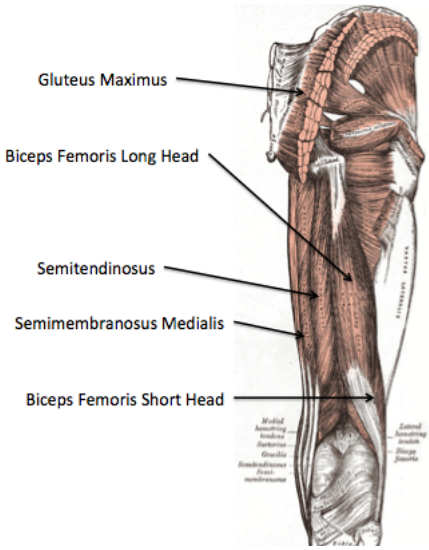

Figure 9: Illustration of the hip extensors and knee flexors [19].

gether with *gluteus maximus* form the hip extensor muscle group. Gluteus maximus is the strongest muscle in the body. The muscles that contribute most to hip flexion are the *iliopsoas* muscle and the rectus femoris. The iliopsoas muscle is a compound muscle consisting of *psoas major*, *psoas minor* and *iliacus*. Iliopsoas muscle is a biarticular muscle attached to the thigh and to the lumbar spine, therefore it acts to flex both the hip and the trunk [11].

2.1.8 Strengthening of a Muscle

Strength can be defined in a mechanical way, the definition is then maximum isometric moment at a predetermined angle. However, usually, strength is measured by moving an external load through a range of movement. Development of muscle strength focuses on increasing the CSA of the muscle and increasing the tension per unit of the CSA. Greater CSA correlates to a greater strength and mass of a muscle [20]. A greater CSA, caused by resistance training, is explained by an increased size of the muscle fibers and increased number of capillaries to the muscle. This generates a greater mean muscle fiber area and separations of myofibrils [11].

2.1.9 Muscle Atrophy

Decrease of muscle mass is the definition of muscle atrophy. The muscle mass is related to the amount of force that can be exerted by the muscle. Hence muscle weakness will occur when suffering from muscle atrophy. On earth, many muscles are activated in order to maintain and stabilize the posture. The muscle needs to work against the external gravity force in order to perform movement and keep the body posture. Being in a microgravity environment will lower the level of force needed for movement and posture stabilization. Thus the muscles do not have to produce as much force as they do on earth. Therefore, there will be a decrease in the muscle activity level. Studies have shown that astronauts traveling in microgravity from five to 11 days suffer up to 20 % loss of muscle mass [21]. Intensive exercise is the only way to minimize muscle atrophy in space, especially, resistance exercise combined with a proper diet. Today astronauts spend at least two hours per day on exercise [21].

2.2 The Flywheel Principle

A spinning wheel or disc with one fixed axis is called a flywheel. A flywheel stores energy in the rotor as rotational energy, which is a form of kinetic energy and can be described with equation 1.

$$E_k = \frac{1}{2} I \omega^2 \tag{1}$$

where ω is angular velocity and I is moment of inertia [22].

Inertia is the property keeping a body moving once it is set in motion [22]. Moment of inertia is described as the moment needed to reach a desired angular acceleration around a given rotational axis. If a flywheel has a higher moment of inertia the disc will spin more slowly for a given energy input. Hence, a flywheel with a lower moment of inertia will spin faster for the same energy input. The moment of inertia for the disc depends on the geometrical form. The given moment of inertia for a:

- solid cylinder is $I = \frac{1}{2} m r^2$
- thin-walled empty cylinder is $I = m r^2$
- thick-walled empty cylinder is $I = \frac{1}{2} m (r_{external}^2 - r_{internal}^2)$

where m is the mass and r is the radius of the disc [22].

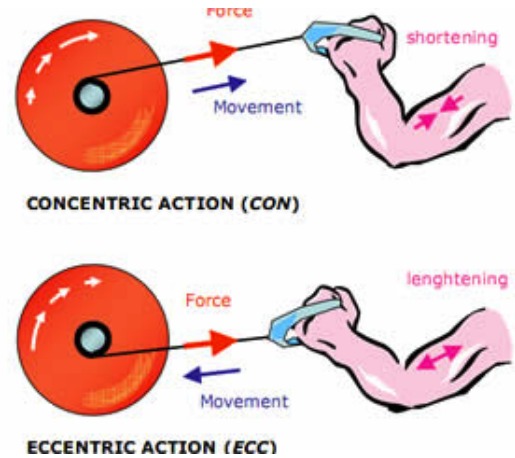

Figure 10: The flywheel technique, showing the muscle activation in the winding and unwinding phase during a biceps curl. The blue arrows represent the direction of the movement. The red arrows represent the direction of the applied force. Image courtesy to YoYo Technology AB [7].

The flywheel exercise device (FWED) is a resistance exercise device that applies the said technique of the flywheel. FWED uses a flywheel instead of weight plates and other instruments that rely on gravity. A strap is winding and unwinding around the flywheels axis. At the other end, the performer is connected to the strap via a harness. When the performer is pressing with the legs to overcome the moment of inertia the wheel is accelerating and the strap is unwound. When the strap is fully unwound at the turning point, the flywheel will start to pull in the strap and wind it up again. The performer then has to decelerate the flywheel. The more force stored in the flywheel during the unwinding phase, the more force is needed to decelerate the wheel in the winding phase [7].

In the unwinding phase, the lower extremities work with a concentric muscle action, the force and movement are working in the same direction. In the winding phase the force is working in the opposite direction compared to the movement, hence, the muscle activity is eccentric. The unwinding and winding phases during a biceps curl are illustrated in figure 10 [7].

2.3 Squat and Flywheel Exercises

Squat and leg press are two exercises, which activate the same muscle groups in the lower extremities.

The first phase of a squat exercise is the down phase. In this phase the performer starts in a standing position, see figure 11. From the standing position, the performer starts to descend towards the ground. First, the performer starts lowering the torso by flexing the hip and knee joints simultaneously, this is done by an eccentric muscle action. When the performer has come to the turning point he or she starts to raise back into starting position by extending the hip and knee joints, this is done by a concentric muscle action.

A leg press is similar to a squat in the sense of what muscle groups are

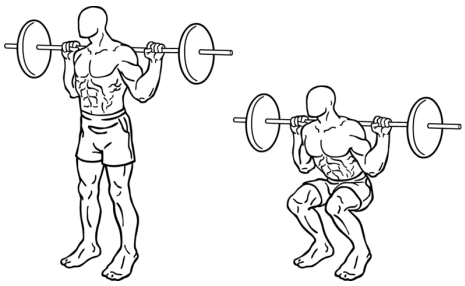

Figure 11: A squat performed with a barbell showing the starting position and the turning point position [23].

Figure 12: The figure shows the inner turning point, before starting the concentric phase. Image courtesy to YoYo Technology [24].

activated and their muscle action types. A leg press on a FWED is performed by pulling a flywheel via a strap. The performer is connected to the strap via a harness. In the starting point, the strap is wound up on a flywheel axis. The performer is sitting on a slider with the feet placed parallel to each other and with the strap between the feet, figure 12 shows the starting position. The performer then starts to press with the legs by extending the hip, knee and ankle joints, resulting in unwinding of the strap. By this action, energy is stored in the flywheel caused by a concentric muscle action. When the strap is fully unwound, the stored energy will start to wind up the strap. The performer must then decelerate the strap by an eccentric muscle action and the hip, knee and ankle joints flexes.

2.4 Biomechanics of Human Movement

The branch in science concerning forces acting on the human body and the effects produced is called biomechanics. Biomechanical theory is based on classical mechanics where the complex system of the human body is simplified. One type of modeling is called rigid body modeling. The body parts are then illustrated as rigid bodies, called segments, where the segments' different masses are concentrated at the segments center of mass [25]. Joints are represented by frictionless hinge joints between segments and the air friction is neglected or assumed to be minimal [26]. Biomechanical analysis can be done from two different perspectives called *kinematics* and *kinetics* [27][11].

2.4.1 Kinematics

Kinematics deals with motion from a temporal and spatial point of view and is often known as "the study of the geometry of motion". Forces, as the source of motion, are not considered in a kinematic analysis. A moving object is described by its height, distance travelled and speed, hence the interesting parameters in a kinematic analysis are position, velocity and acceleration [11]. It is possible to calculate the range of the shot by studying the initial conditions of projection speed, angle and height difference.

2.4.2 Kinetics

The other perspective of biomechanical analysis, where all forces causing the motion is considered, is termed kinetics. Both external and internal forces are considered. Kinetic studies are significant when examining human motion, even static positions and postures, as all motions are controlled by forces produced by the body.

As mentioned before, a system of the human body can be either static or dynamic. To analyze these, either static or dynamic analysis is used. Dynamic analysis is generally used to model a system of the human body where accelerations are acting on segments. Forces of different types are present in such a system (gravitational force, contact force, muscular force and inertial force caused by the acceleration) and therefore makes it more complex to analyze. However, the forces can be determined by assessment of the motion which was analyzed kinematically.

The technique to determine the forces by evaluating the motion, is called Inverse Dynamics (ID). ID is also commonly known as the "Newton-Euler inverse dynamics approach" and is based on Newton's second law of motion

$$\overline{F} = m\overline{a} \tag{2}$$

and Euler's law of motion

$$\overline{M} = I\overline{\alpha} \tag{3}$$

where $\overline{F}$ is force, m is mass, $\overline{a}$ is linear acceleration, $\overline{M}$ is moment, I is moment of inertia and $\overline{\alpha}$ is angular acceleration. In this way the forces and moments can be calculated from the accelerations. An example of a free body diagram used in an ID study can be seen in figure 13.

This type of ID represents a simplified model of a biomechanical system. In reality, it is a much more complex system where muscles consist of soft tissue wrapping around each other and other anatomical parts, creating interactions which are simplified in ID. The muscles are performing work on the segments creating applied forces on many points, thus creating different

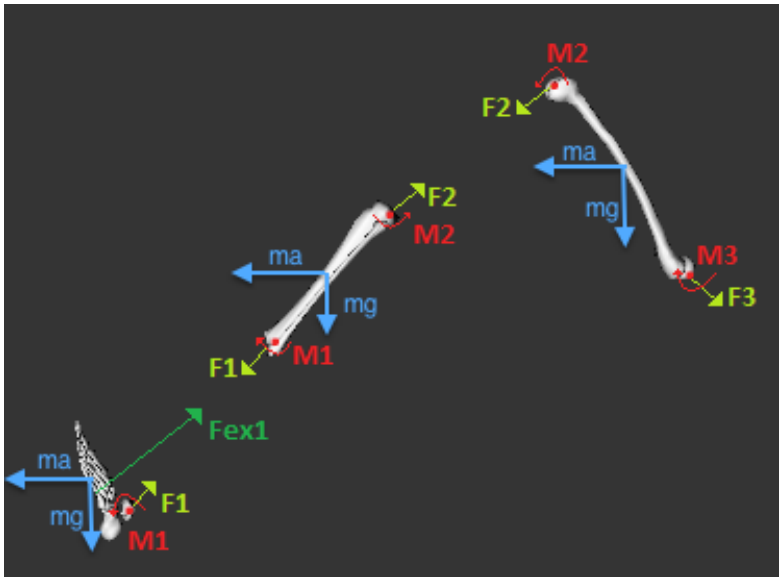

Figure 13: The picture shows an illustration of the forces acting on a lower limb. The contact force is represented by the ground reaction force, $Fex1$, and the internal joint forces and moments are represented by F and M respectively. Each segment has a mass m and the gravitational force g is acting upon them. Furthermore, the segments are moving with a linear acceleration a.

lever arms, all affecting the internal joint forces. ID only considers the internal joint reaction moment as a sum of separate muscle moments. Therefore no indication of which muscles, and to what extent they are activated, is given. Neither does it reveal whether there is any co-contraction or not. Hence, to analyze the individual muscle effects and more precise joint forces and moments, it is necessary to use more complex modeling systems in order to get a model closer to reality [25]. There are several biomechanical modeling softwares on the market that can be used for this application, two of them are AnyBody Modeling System [25] and OpenSim [28].

2.5 Biomechanical Analysis

To perform a biomechanical analysis, experimental sessions can be performed in order to gather data of a specific motion. There are many variables and parameters that can be of interest and they vary with the type of project. One important parameter in all biomechanical analyses is the anthropometric data of the test subject, i.e. the anatomical measurements of the specific individual. Furthermore, segmental kinematics, external forces and muscular activity can be useful variables in an analysis [29].

2.5.1 Segmental Kinematics

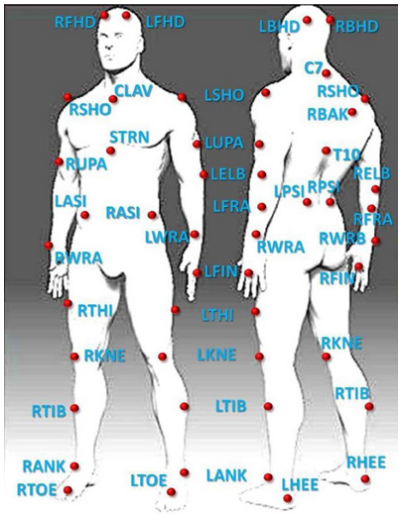

Figure 14: An example of reflective markers placed on anatomical landmarks on a human test subject [30].

In order to collect kinematic data, a method called *motion capture* can be used. The concept of motion capture is translation of an analog motion into digital data. This can be done in several ways where the two most commonly used methods are the *marker-based* and the *marker-less* optical motion capture systems. The marker-less motion capture system is based on computer vision technology. The technology uses advanced algorithms in order to calculate trajectories from the object, without having any specific markers to track. The marker-based motion capture system uses markers which are tracked. The markers are often retro-reflective balls or lights and are placed on anatomical landmarks, often at the positions seen in figure 14. In this report they are also referred to as *experimental markers*.

Several cameras are placed around the subject to create a three dimensional space where the markers can be tracked, as can be seen in figure 15. At least two cameras have to register a marker in order to compute the position in the space. The cameras register the trajectory of the markers in a global coordinate system over time, assigning coordinates to each marker in three dimensions for every instant of time [31][32].

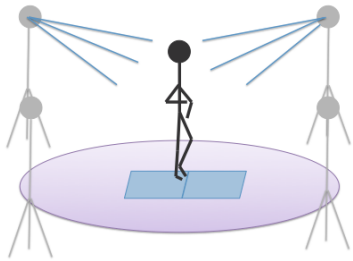

Figure 15: Cameras used in marker-based motion capture are placed around the experimental area where a test subject is walking over integrated force platforms.

2.5.2 External Forces

External forces need to be known in order to perform a kinetic analysis of a biomechanical system. They can be measured in many ways, for example, by a strain gauge, a spring scale or a force platform. Force platforms, or force plates, are devices measuring reaction forces. As can be seen in figure 15, force plates are often integrated in the floor in gait labs where the reaction forces from standing, walking, running or jumping etcetera are measured [11]. There

also exist portable force plates which can be moved and applied to different experimental setups. There are many different kinds of force platforms which can give varying outputs but the main function is the same. Force plates use transducers to distinguish and convert the applied pressure into three force components in its local frame. The force plates are also able to register the centre of pressure, which is the point of action of the ground reaction force [29].

2.5.3 Muscular Activity

Electromyography (EMG) is the measurement of the electrical signals produced by the muscles during activation. The electrical signal measured is the change in muscle action potential, which is created when a neuron is stimulating the muscle fiber [11]. It is common that EMG is collected from one or several muscles which are crucial when performing a specific movement interesting for the study. EMG gives an indication of when certain muscles are active and muscle fatigue can also be shown. There are two types of EMG; surface EMG and intramuscular EMG. Surface EMG uses electrodes applied on the skin which detects the electrical signal produced by the muscle. Intramuscular EMG uses needle electrodes which are inserted directly into the tissue of the targeted muscle [29]. EMG can also give an indication of produced muscle force, however more studies are needed to confirm an explicit relationship [11].

2.5.4 Simulation Software

As mentioned in section 2.4.2, one way to analyze more complex biomechanical systems is to use a biomechanical simulation software. One software which is designed to analyze musculoskeletal systems is the license software *AnyBody Modeling System* (AnyBody Technology A/S, Aalborg, Denmark). A model created in AnyBody can, besides the musculoskeletal system, include external loads, objects and specifications of motions. An example of a human musculoskeletal model interacting with an object can be seen in figure 16 where the entrance and exit of a car is modeled.

The AnyBody software uses text based modeling through a programming language called AnyScript. The AnyBody Modeling System can be used to create a model from scratch or to modify already existing models. The existing models are collected in a library called The AnyBody Managed Model Repository (AMMR). Models for different purposes can be found in the AMMR and more are added successively [25].

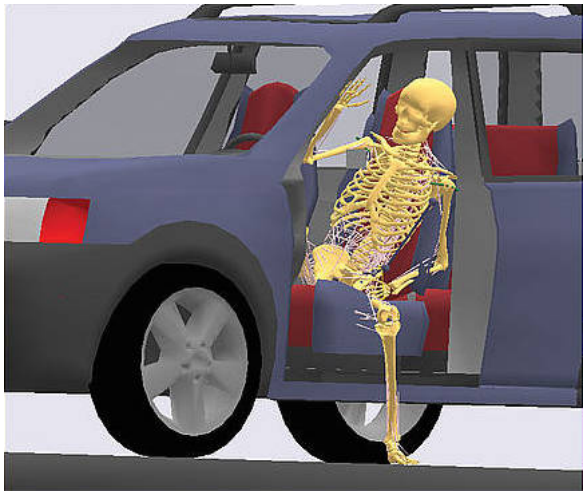

Figure 16: Modeling of stepping in and out of a car with the AnyBody Modeling System. Image courtesy AnyBody Technology [33].

One model found in the AMMR is the *MoCapModel* which can be used when input data from motion capture is available. The MoCapModel uses anatomical data from The Twente Lower Extremity Model (TLEM). TLEM is a model of a human based on studies of a male embalmed specimen [34]. The MoCapModel models 55 muscles in the lower human body by 159 representational fascicles per leg [35].

The AnyBody modeling system uses two steps to complete the biomechanical analysis. The first step is the kinematic analysis called *Motion and Parameter Optimization*, also referred to as *scaling of the model* in this report. During this step the model is adjusted to match the anthropometrical data of the test subject and the desired motion, collected during a motion capture session. Through optimization, the segment lengths, joint centers, joint axes and marker positions are determined in the way that they have the best match to the recorded motion. This is done by several cycles where the default markers of the AnyBody model are moved, little by little, to agree with the experimental marker positions. The output from this step is joint angles [36][25].

The second step is the kinetic analysis called *Inverse Dynamics*. In this step external forces are applied, for example from collected reaction force data. The Inverse Dynamics step is based on the basic principles of inverse dynamics (ID) (described in section 2.4.2) and calculates internal net joint moments and muscle activity. However, AnyBody also takes the effect of muscles and tendons into account.

The fact that the model consists of many muscle representations results in a redundancy problem. This is because of the infinite number of muscle recruitment patterns which can satisfy the desired movement. To solve the redundancy problem AnyBody uses an optimization problem where the total representation of muscle force is minimized. This is based on the assumption that the Central Nervous System (CNS) has the strategy of achieving maximum synergism (when the muscles are helping each other as much as

possible). The force equation of the system is represented by the following equation

$$\boldsymbol{C}\overline{f} = \overline{d} \tag{4}$$

where $\overline{f}$ represents both the internal joint reaction forces and muscle forces ($\overline{f} = [\overline{f}^{(R)T}\overline{f}^{(M)T}]^T$), $\boldsymbol{C}$ represents a coefficient matrix and $\overline{d}$ are the known applied external forces [25].

3 Method

Two exercises have been studied in this pilot study. The first was a leg press performed on a FWED and the second was a conventional squat with only bodyweight. Two different test subjects were performing one type of exercise each. The FWED leg press was performed by a 40 year old female subject with a height of 164 cm and a weight of 61 kg. She was in good physical shape, but was not familiar with performing a leg press on the FWED. The squat was performed by a 25 year old male subject with a height of 171 cm and a weight of 65.7 kg.

Marker-based motion capture technology with retro-reflective markers was used during both studies, as well as detection of reaction forces. Additionally, EMG data was collected for the rectus femoris muscle during the performance of a squat in order to validate the created computerized musculoskeletal model. The collected data was then used to perform biomechanical simulations and analyses of the two systems. The simulations were done with the licensed software AnyBody Modeling System. Three different conditions were simulated:

- FWED1 - a FWED leg press in earth gravity,
- FWED0 - a FWED leg press in micro gravity,
- Squat - a squat in earth gravity.

Simulated data of joint angles, net joint moments and muscle activation was extracted from the software and plotted for analyses.

3.1 Laboratory Sessions

Biomechanical data was collected during two lab sessions, they are referred to as the FWED leg press session and the squat session.

3.1.1 FWED Leg Press

An earth-based exercise session was performed in a motion laboratory at *Karolinska Institutet, Institutionen för neurobiologi, vårdvetenskap och samhälle* in Huddinge, Sweden, in July 2014. The exercise performed was a leg press on a prototype of the FWED YoyoMultigym [24] using two flywheels with a total moment of inertia of 0.0811 kgm^2. Figure 17 shows the setup of the YoYoMultigym in the laboratory with the test subject performing a leg press. The motion capture system used was BTS Elite (BTS Bioengineering, Milano, Italy). 8 cameras were placed around the test subject and sampled at

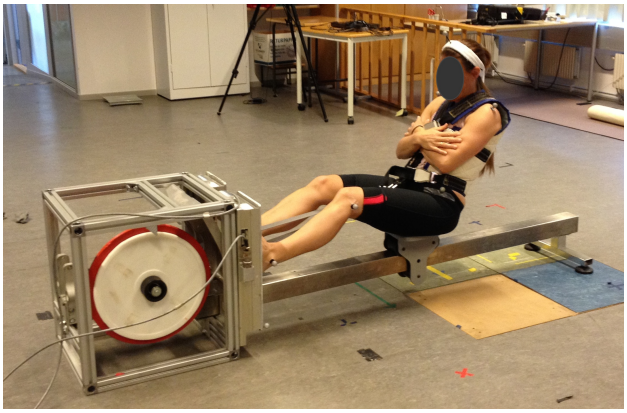

Figure 17: The figure shows the laboratory setup of the YoYoMultigym. Two flywheels (red and white) and force plates are attached to the device.

a frequency of 100 Hz. 14 markers were placed on the subject at the specific landmarks stated in Appendix D. The positions were chosen so that joint centers and body segment lengths could be determined. The test subject was wearing a vest where the strap to the flywheel axis was attached (see figure 17).

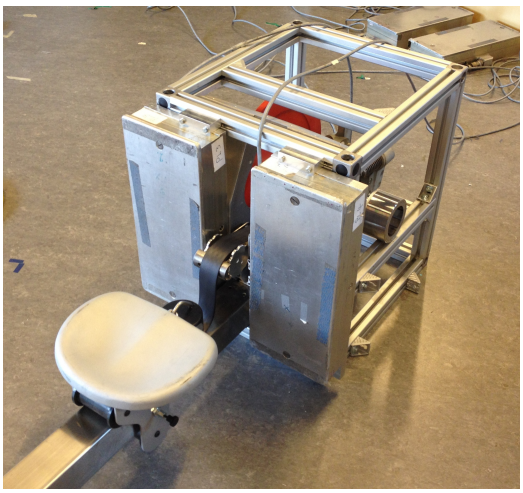

Figure 18: The AMTI force plates were attached to the frame of the Multigym.

Two movable AMTI MC818 force plates (Advanced Mechanical Technology Inc., Watertown, Massachusetts, USA) were used in order to measure reaction forces from the feet during a leg press. The transducers sampled at a frequency of 100 Hz. A preparation of the frame of the YoYo Multigym was done to allow attachment of the force plates. Two separate parts were constructed and manufactured in the workshop at STH KTH (Flemingsberg, Sweden). A detailed view of the parts and the attachment can be seen in Appendix A. The final setup can be seen in figure 18, where the force plates are mounted with a 90 degree angle relative to the floor.

The test subject had a short familiarization session before the sampling started. The sampling was initialized when the test subject felt comfortable with the exercise and had attained a flow in the movement. Then, 20 seconds

of sampling took place while the test subject performed repetitions of leg presses continuously.

3.1.2 Squat

The squat session was performed in the motion laboratory *Motoriklab* at *Astrid Lindgrens Barnsjukhus*, Solna, Sweden, in October 2013 . The exercise performed was a bodyweighted squat and data was collected during one squat.

The motion capture system used was Vicon MX40 (Vicon, Oxford Metrics Ltd, UK). The system consisted of 8 cameras sampling at a frequency of 100 Hz. 26 reflective markers were used and placed at the positions stated in Appendix E.

Two Kistler 9281C force plates (Kistler Holding AG, Winterthur, Switzerland), integrated in the laboratory floor, were used. The force plates were used to collect ground reaction force data during the squat where the test subject had one foot on each platform. The sampling frequency was 1000 Hz. Furthermore surface EMG of rectus femoris was collected during the session using a Noraxon wireless EMG system (Noraxon, Scottsdale, Arizona, USA).

3.2 Data Formatting

The BTS Elite motion caption system and the AMTI force plates produced data in formats (.ric and .gr*) which was incompatible with the AnyBody software (.c3d). Thus conversion of the .ric and .gr* files had to be done. The open-source software Mokka, which is based on the open-source Biomechanical ToolKit (BTK), has the ability to import several biomechanical laboratory data formats and then export it into a different format. Mokka was therefore used to create a .c3d file consisting of motion capture data and force plate data from the FWED leg press session. As the data from the force plates was in a local coordinate system it had to be transformed into the global frame of the motion capture system. This was done by editing the .c3d file manually, using MATLAB (MathWorks, Natick, Massachusetts, USA) and BTK.

The EMG data collected from rectus femoris during the squat was processed in order to make it comparable to simulated muscle activity. The signal was processed using full-wave rectification, removal of DC offset and generation of the linear envelope. This was done in MATLAB and the programming code can be found in Appendix B.

3.3 Simulations

In order to analyze the biomechanics of the two systems a musculoskeletal model was created by using the simulation software AnyBody Modeling System 6.0.3 (AnyBody Technology A/S, Aalborg, Denmark). The Lower Body of the MoCapModel (AMMR 1.6.3) was used and modified to create a musculoskeletal model, corresponding to the anthropometrical data of the two test subjects. The AnyBody software allows simulation of the systems in a microgravity environment.

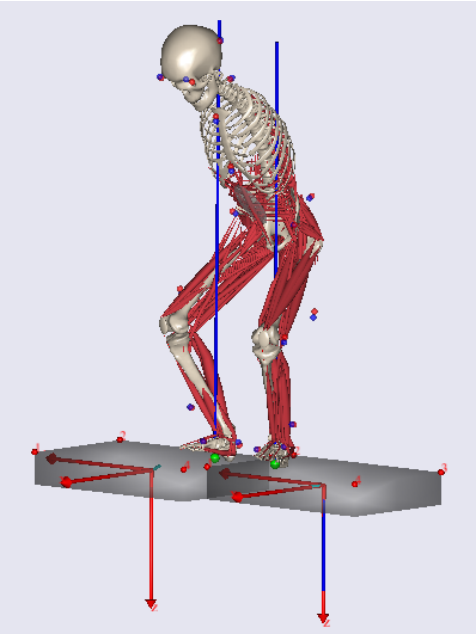

Figure 19: The figure shows a print screen of the squat system modeled in the AnyBody software. The gray blocks represent force plates and the blue arrows going from the feet up in the body are reaction force indicators.

The MoCapModel was modified in a few ways to comply with the FWED leg press. First, the number of markers needed to be adjusted since fewer experimental markers were used than what was represented in the MoCapModel. The coordinates of the models marker positions were also adjusted to match the experimental setup as much as possible. The number and position of markers used during the squat session agreed exactly with the model in AnyBody and therefore no adjustments of markers were necessary for the squat model. An illustration of the MoCapModel customized to the squat is shown in figure 19.

To drive the model, the data collected from the motion capture sessions was used. The data was stored in .c3d files, where both experimental marker coordinates and reaction forces were to be found. This .c3d file was read by the AnyBody model in the Motion and Parameter Optimization study and the Inverse Dynamics study. In the Motion and Parameter Optimization study the marker coordinate data was used and in the Inverse Dynamic study the force plate data was used.

The AnyScript of the MoCapModel needed to be adapted to the type of force plate used, as there are many different types giving various output data. The motion lab where the squat was performed had force plates of a type which was possible to integrate in AnyBody using an existing class

template. However, the AMTI force plates used during the leg press on the FWED are less common. Therefore a new force plate class template was programmed, the script can be seen in Appendix C.

An estimation of the traction force, acting on the test subject through the vest and the strap, was done. The traction force was modeled as a point force at sternum, acting in the opposite direction of the sum of the reaction forces from the feet (see figure 20). As the system is a closed loop the magnitude of the traction force was assumed to be the same as the sum of the reaction forces measured by the force plates.

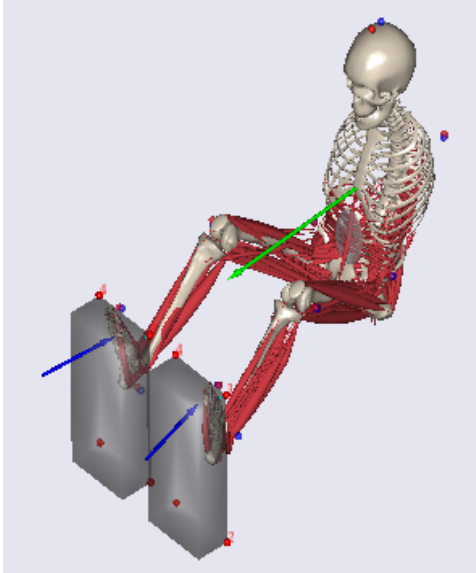

Figure 20: The figure shows a print screen of the FWED leg press system modeled in the AnyBody software. The gray blocks represent force plates with blue arrows showing the reaction force. The green arrow represents the traction force produced by the pulling of the flywheels.

After these modifications. the model was ready to simulate the three conditions, the FWED leg press in earth gravity and micro gravity and the squat. To simulate earth gravity, a gravity constant of 9.81666 m/s^2 [37] was used, and to simulate micro gravity, the gravity constant was set to 0 before computing the Inverse Dynamics study.

AnyBody produces simulated results in joint force and joint moment but not joint power. As the power was of interest for the study the joint power was calculated by the equation

$$P = \overline{M} \cdot \overline{\omega} \tag{5}$$

where P is Power, $\overline{M}$ is Moment and $\overline{\omega}$ is angular velocity.

4 Results

As both the FWED leg press and the squat were symmetric motions it has been chosen to only present the results of the left leg. Angles, moments, powers and simulated activities presented here are all results achieved from the AnyBody Modeling System, where the simulated activity is the ratio of the actual muscle force with respect to its theoretical maximum capacity. In the analyses of activities only FWED1 and FWED0 was considered.

4.1 Reaction Force

Figure 21 shows the reaction forces collected during the laboratory sessions. The reaction force from the Squat was relatively constant through the whole motion. The reaction force from the leg press on the FWED varied with lesser force in the beginning and at the end of the motion. Maximum force was seen in the middle of the leg press, i.e. in the innermost point when the strap was fully wrapped up. The magnitudes of the two reaction forces were somewhat similar, with the FWED leg press showing a maximum force of a little above 400 N and the squat just under 400 N.

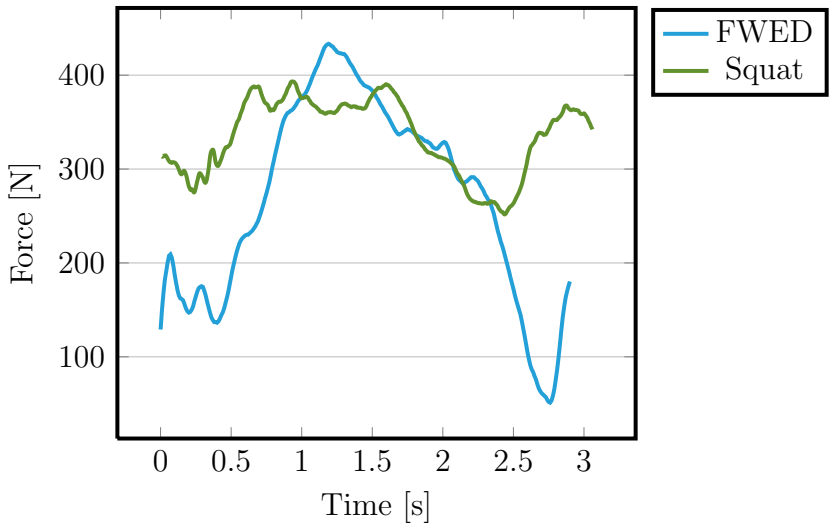

Figure 21: Reaction force of a FWED and a squat.

4.2 Simulated Activity vs. Measured EMG

Figure 22 shows a comparison of measured EMG data of rectus femoris and simulated activity of rectus femoris, both from the squat. The left axis shows

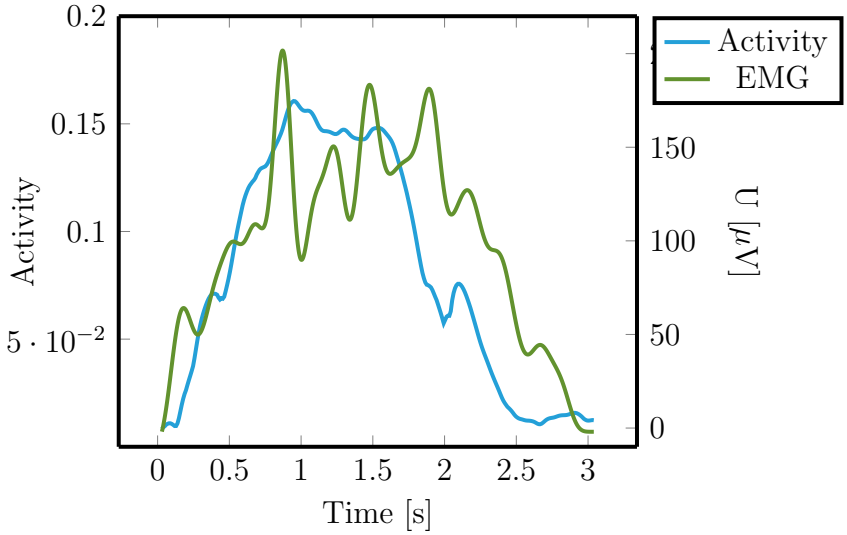

Figure 22: Plot showing simulated activity and measured EMG data.

activity and the right axis shows the EMG in microvolt (μV). The activity of rectus femoris reached about 15 % of its maximum capacity and the muscle contributed to the motion during the whole movement, especially in the middle, i.e. the lower turning point. The activity and the EMG follows the same trend.

4.3 Ankle Joint

The three plots in figure 23 show ankle joint angle, ankle joint moment and ankle joint power respectively. Every plot shows three representations, the representations are from the FWED leg press in earth gravity (FWED1), FWED leg press in zero gravity (FWED0) and the Squat.

The angles of FWED1 and FWED0 were the same and had a variation of 64 degrees throughout the motion. The squat varied with around 35 degrees. All three cases were showing a dorsiflexion of the foot but the squat showed a larger dorsiflexion at all times.

As in angles, the moments of FWED1 and FWED0 were the same. They were plantarflexing and getting bigger in the middle of the motion. The ankle moment of the squat was very small and was changing insignificantly.

The plots of ankle joint power of the FWED1 and FWED0 were showing an absorption during the first half of the leg press and then a concentric action generating power in the other half. There were few oscillations in power during the leg press. The Squat also showed absorption followed by generation of power, however, to a significantly smaller extent.

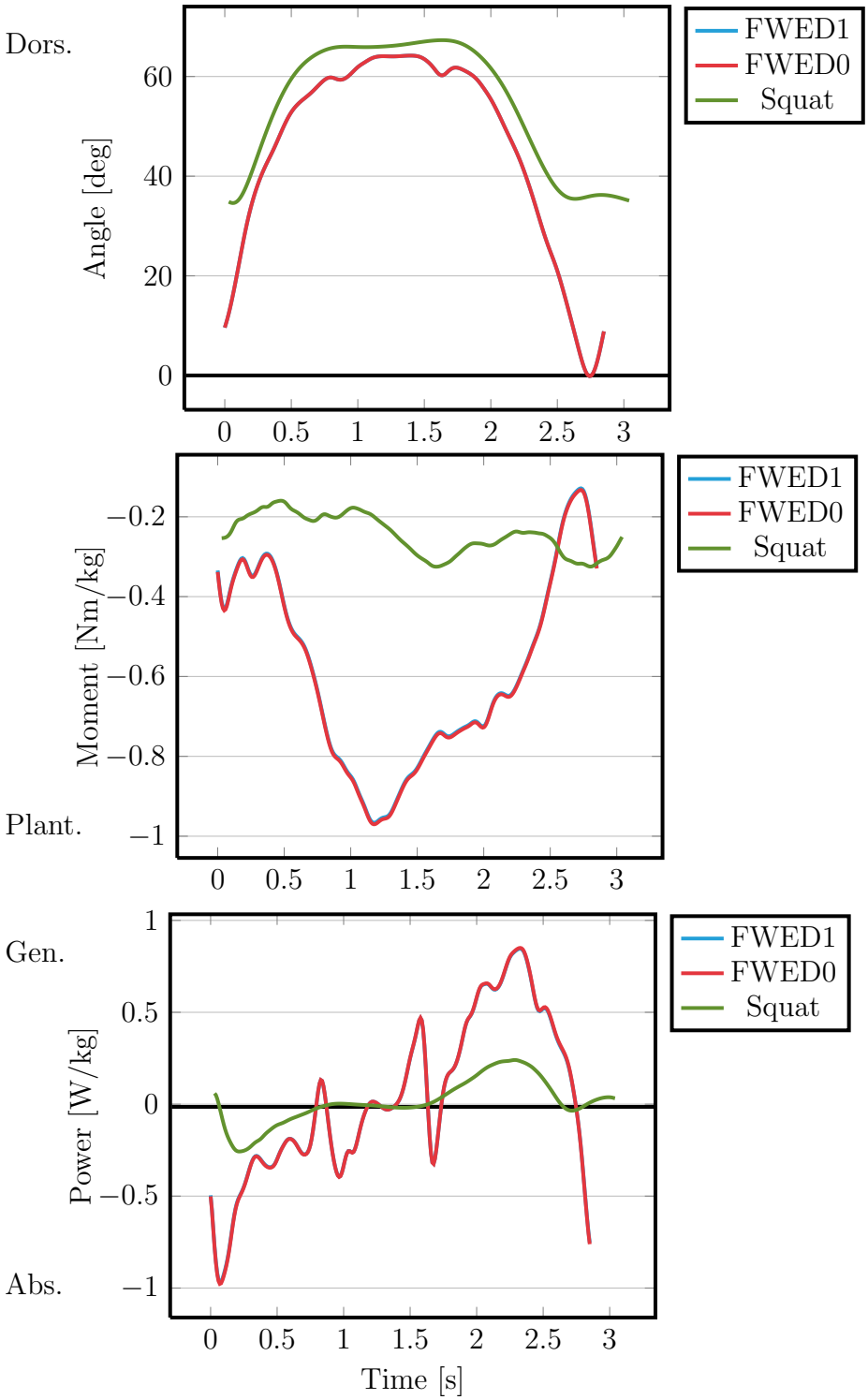

Figure 23: Plots showing angle, moment and power of the ankle joint.

4.4 Knee Joint

The three plots in figure 24 represent angle, moment and power of the knee joint for the three cases FWED1, FWED0 and Squat.

The knee angle of FWED1 and FWED0 were the same and varied from 17 to 105 degrees of flexion. The knee was flexed for the squat during the whole motion, starting at 15 degrees and reaching a maximum flexion of 140 degrees. The flexion of the knee during the squat was bigger than during the FWED leg press.

The moments of all three cases were rather similar in the knee joint. There were extending moments during the majority of the motions. However, when the motions started and ended there were flexing moments in all cases.

The power in the knee joint showed some oscillations for FWED1 and FWED0. Unlike the ankle, there was a small generation of power in the beginning before the eccentric motion started in the FWED leg presses. Then it followed the same pattern as the ankle with the rest of the first half absorbing power and the second half generating. The squat was absorbing power directly from the beginning. The absorption and the generation of knee joint power was bigger during the squat exercise than during the leg press in both 0 and 1 gravity.

4.5 Hip Joint

The plots in figure 25 illustrate the angle, moment and power of the hip joint. The angles of FWED1 and FWED0 were, as in the other cases, identical. The hip angle during the leg press varied with 40 degrees. The squat showed a bigger variation of almost 105 degrees. All cases showed a hip flexion during the whole simulation.

The hip joint showed a difference of approximately 0.4 Nm/kg in amplitude between the FWED1 and FWED0. However, the two had the same shape of curve. The moment from the squat showed a slightly different shape than the leg presses but reached a similar amplitude and varied similar to FWED1. All moments were extending, except for FWED1 right in the beginning and at the end.

The FWED1 showed a power curve with a little absorption during the first half and a little generation during the second half. FWED0 showed a similar curve with a slightly greater amplitude. The squat showed higher amplitudes in both absorption and generation than any of the FWED leg presses.

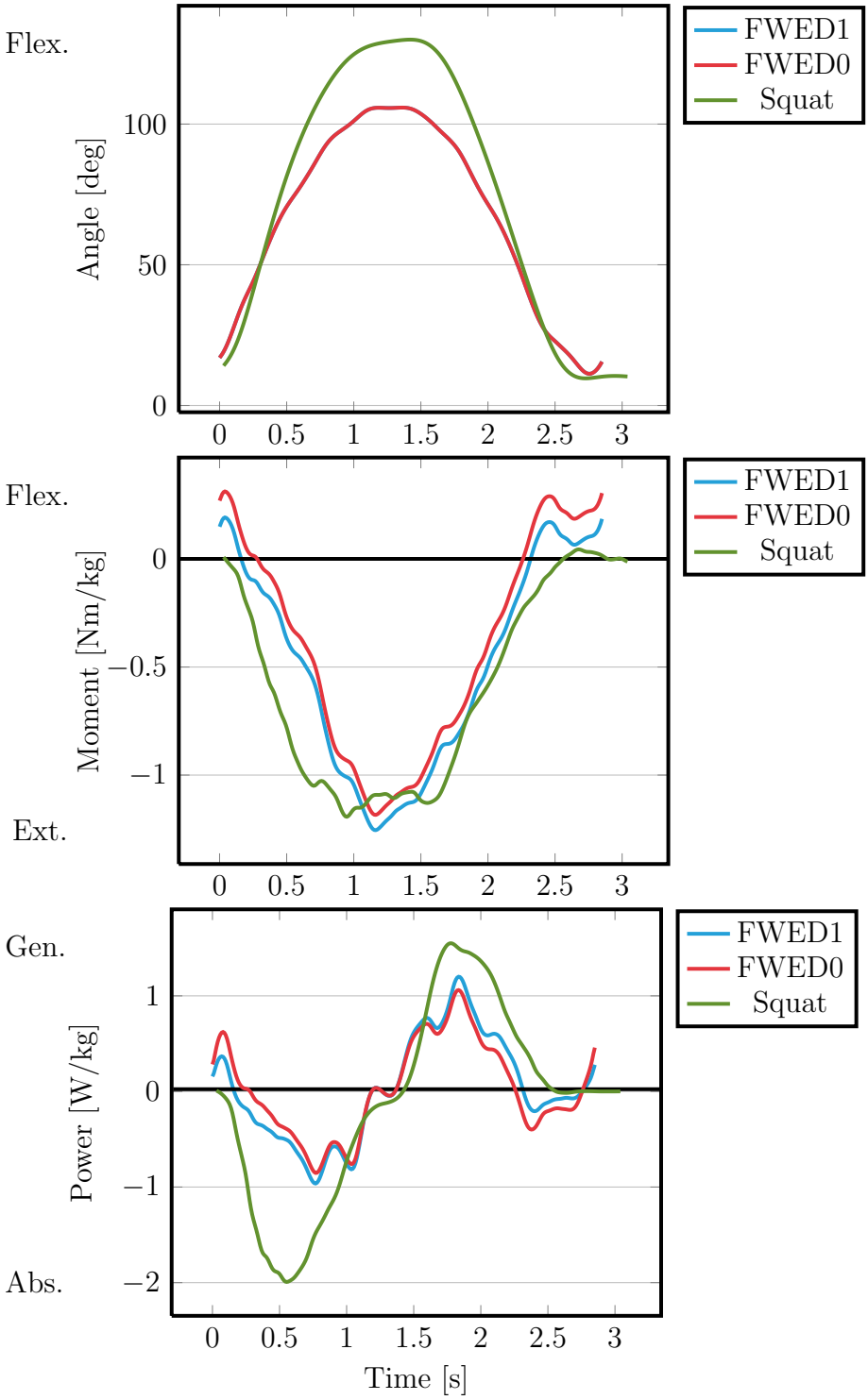

Figure 24: Plots showing angle, moment and power of the knee joint.

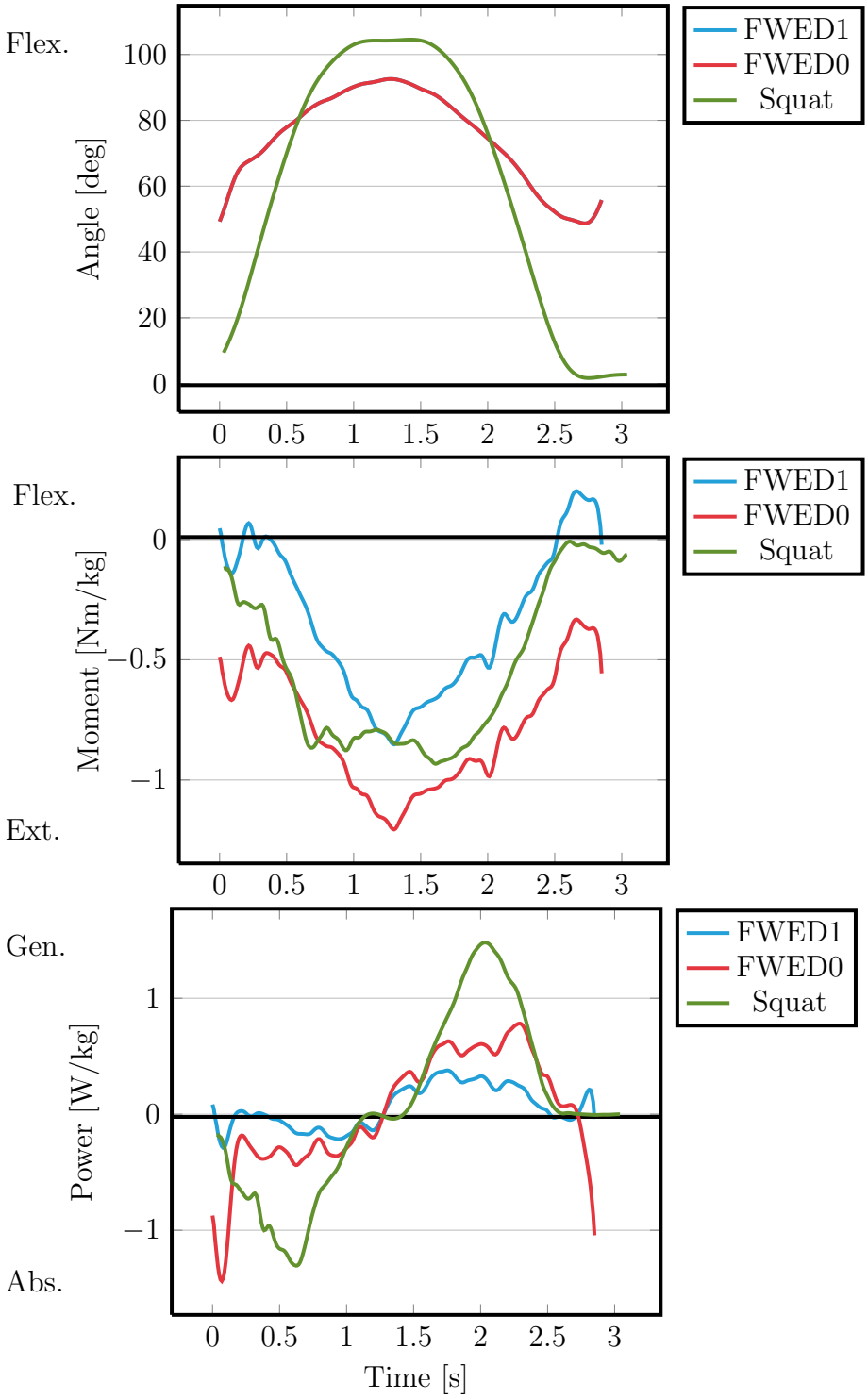

Figure 25: Plots showing angle, moment and power of the hip joint.

4.6 Simulated Activity

Figure 26 shows the activity of ankle plantarflexors. Small activities in the gastrocnemius muscles was seen in the beginning of the cycle, thereafter the activity increased with a peak in the inner turning point. The activity thereafter decreased as the performer was going back to the outer turning point. For the soleus muscle, activation was seen in the beginning and at the end of the cycle, with no activation in the middle. The highest activity was found in gastrocnemius medialis in 1g in the inner turning point, with a peak around 37 %. A small dip occurred in the gastrocnemius muscles after the inner turning point, on the way back to the outer turning point. There were no significant differences between the two gravity conditions for any of the muscles.

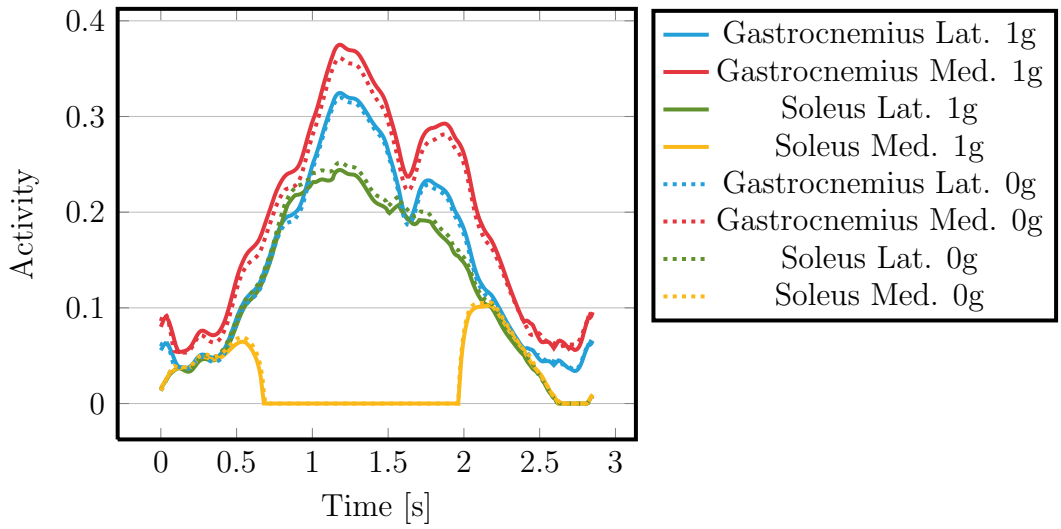

Figure 26: Activity of ankle plantarflexors.

Figure 27 shows the activity results of the knee extensor muscles. No indication of activity was seen at the starting point. The activity smoothly increased for all knee extensors as the performer approached the inner turning point. The activity decreased as the performer returned to the outer turning point, with a small dip around 1.7 s. The highest activity occurred in Vastus Lateralis in 0g, with a peak value around 55 %. The two different gravity conditions were relatively similar with respect to amplitude and pattern.

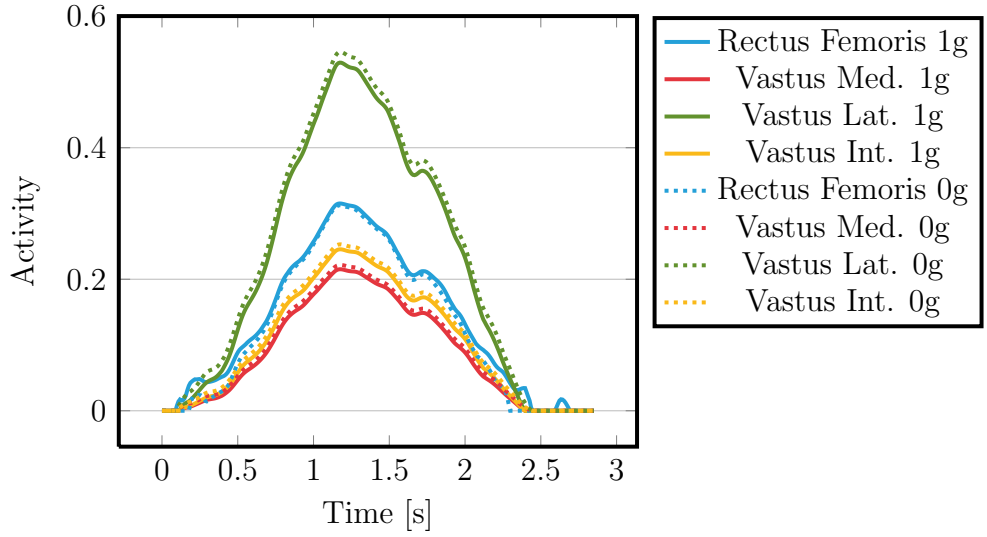

Figure 27: Activity of knee extensors.

Figure 28 shows the activity of the hip extensor muscles. Nearly no activity occurred for the hip extensors in 1g at the beginning of the cycle, while all hip extensors in 0g displayed indications of activity. The activity increased until the inner turning point and thereafter decreased during the return. The curve was relatively unstable with four small dips towards and away from the turning point for all muscles except for the semimembranosus and semitendinosus in 1g. There were notable differences between the amplitudes in the various muscles in the different gravity conditions.

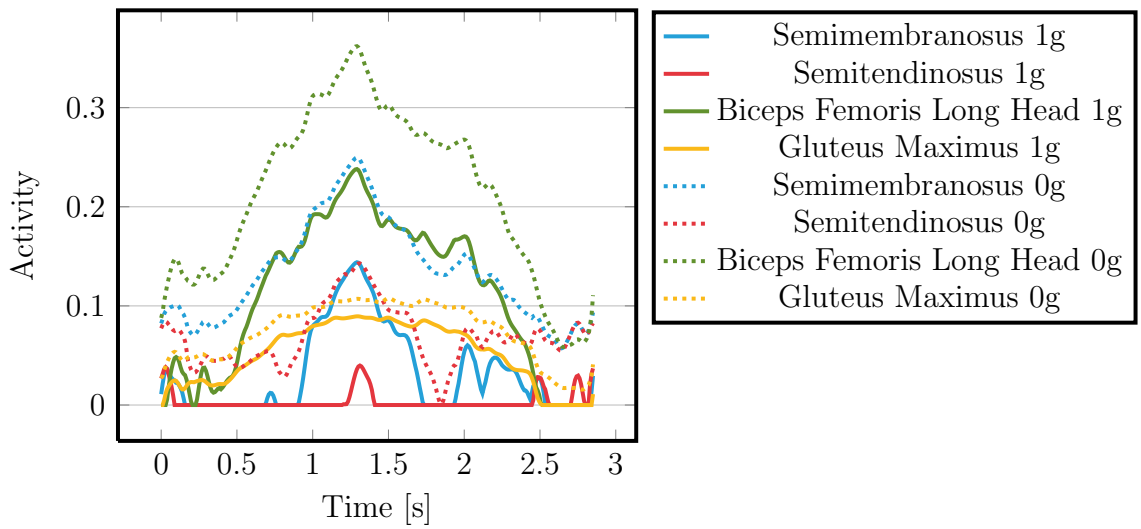

Figure 28: Activity of hip extensors.

Semimembranosus in 0g showed a peak activity around 35 %, while semimembranosus showed a peak activity near 25 %. Semitendinosus in 1g was inactive during the majority of the cycle, with a small activation in the turning point. Semimembranosus was inactive during a period in the first half of the cycle, and also during a short period in the second half.

Figure 29 shows the activity of knee flexor muscles. The only difference from the hip extensor muscles presented was the presence of biceps femoris short head and the absence of gluteus maximus. Biceps femoris short head showed no activity during the majority of the cycle, however, a small activity was seen in the beginning and at the end. See previous paragraph for the explanation of the rest of the knee flexor muscles, as these muscles are also hip extensors.

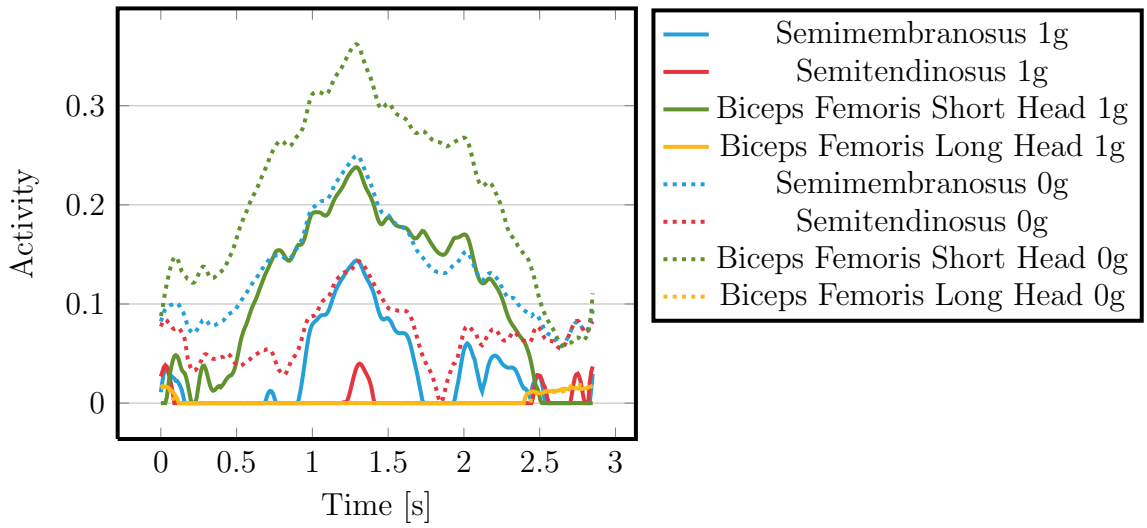

Figure 29: Activity of knee flexors.

Figure 30 shows the activity results of the hip flexor muscles. No notable indication of activation was seen in the iliacus muscles during the cycle. The iliacus lateralis showed a small activity during a shorter period in the beginning and at the end of the cycle. Activation was only be seen in rectus femoris. No significant difference was seen between the two gravity conditions.

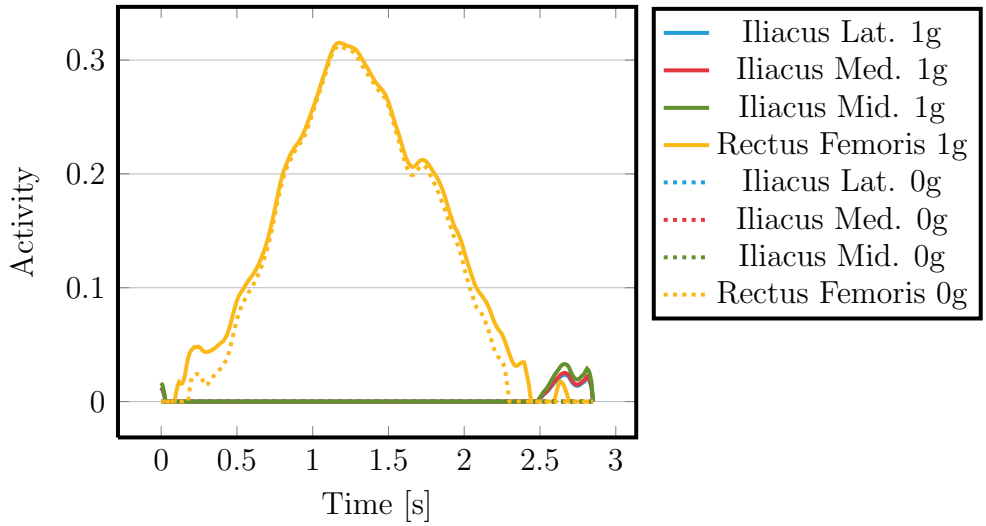

Figure 30: Activity of hip flexors.

5 Discussion

The discussion is divided into three sections starting with the analysis and discussion of results. Furthermore a discussion about the laboratory sessions and the modeling in AnyBody is presented.

5.1 Results

5.1.1 Reaction Forces

The reaction forces collected from the two different exercises differed in shape. This diversity can be explained by the respective loads in the exercises. During a body weighted squat the external loads affecting the subject are more or less constant, it is only the acceleration of the body creating a variation. However, when performing a leg press on the FWED, the loads will change more throughout the range of motion due to the flywheel effect. This is seen in figure 21, where a lower load occurred in the beginning and at the end of the motion (in the outer turning point) and with the maximum load in the middle (the inner turning point). From a countermeasure exercise perspective for astronauts, a relation between better bone remodeling and varying loads has been shown. One can therefore speculate that exercising on a FWED will give a good stimulation of bone growth.

5.1.2 Simulated Activity vs. Measured EMG

The comparison between computed activity and collected EMG data of rectus femoris for the squat exercise showed some correlation. The two illustrations of muscle activation, seen in figure 22, followed a similar pattern with the same period of excitation. The delay of the EMG signal compared to the activity could be explained by the time it took for the nervous system to send an excitation signal before the muscle was actually excited. It should also be considered that EMG data was exposed by artifacts and noises. Electromagnetic sources from the environment may have obscured the EMG signal for example. Of course it is difficult to compare computed activity to an EMG signal in any detailed manner. However, it can be said for certain that both were activated during the same period and followed a similar shape. From these aspects, the musculoskeletal model in AnyBody was assumed to be valid and acceptable to use for modeling and simulation of the FWED leg press.

5.1.3 Joint Angles, Moments and Powers

All angle plots of the three joints, ankle, knee and hip, showed no difference between FWED1 and FWED0 (see ankle plots in figures 23, 24 and 25). The results computed by AnyBody were based on the same kinematic motion data and external loads, therefore no difference in motion was generated.

However, differences in angles between the FWED and the squat could be seen, indicating the differences between the two motions. The ankle angle plot in figure 23 shows that the squat started with a significantly large dorsiflexion angle, when it was in fact expected to be around zero degrees in an upright standing position. This might have been related to the marker positions making the scaling of the model in AnyBody a bit faulty. However, this was nothing that affected the rest of the results considerably as the feet were constantly flat on the ground. Moreover, the bigger variation in ankle angle for the leg press originated from the heel raise needed during the performance. The experimental setup of the force plates forced the test subject to perform a heel raise.

Furthermore, the fact that no difference could be seen between the two gravity conditions in the ankle joint moment (see figure 23) is probably explained by the fact that the segment mass of the foot was insignificant, especially when the direction of movement was perpendicular to the gravity vector. The heel raise was probably also a big contributor to the remarkable ankle joint moment in a FWED leg press. In a heel raise the only point of contact between the feet and the force plates could be found in the toes, this gave rise to a bigger moment arm creating a bigger moment. In the squat, however, the whole footpad was always in contact with the floor making the lever arm shorter as the centre of gravity is aimed to be somewhere in the middle of the contact area in order to keep the balance. The bigger extending ankle moment in FWED indicates that the plantarflexors (mainly gastrocnemius and soleus) were more active in a FWED leg press than in a normal squat.

As joint power depends on joint moment and joint angle velocity, one could expect that the powers of FWED1 and FWED0 would have been the same. It was also expected that the powers of the leg presses were larger than the power produced during the squat because of the larger variation of angle and larger moment seen in the FWED leg presses. The absorption of power in the first phase of FWED leg press, seen in the power plot in figure 23, is because of the eccentric movement during the winding of the strap on the flywheel axis. Similarly, the generation of power during the second half indicates a concentric action during the unwinding phase. The squat showed the same pattern with an eccentric action in the down phase and

a concentric movement in the up phase. The difference between absorption and generation in a FWED leg press can originate from the cycle performed before, as the results showed only a selection of one cycle. The oscillations of the FWED power curves could be a consequence of the small downtrends seen in the angle graph where the angle velocity decreased and changed direction.

The angle plots of the knee joint, seen in figure 24, showed that the squat produced a larger flexion, i.e. the test person made a deep squat. The fact that the moments in the knee were very similar in all three cases, in spite of different loads, can be explained by the moment being an internal net moment, a net effect of the muscle forces affecting it. The moment of the squat started and ended in 0. This could be due to the static upright position in the start and at the end, where no lever arm acts on the knee joint. The leg press, however, was performed as a continuous dynamic motion and no static position was recorded, therefore a flexing moment could be seen in the start and at the end of the range of motion. Even though the whole leg press required mostly extension in the knee joint the flexion moment could be explained by the test subject getting ready for the recoil and change of direction. As discussed above, the ankle moment during the FWED leg press recruited the plantarflexors in order to complete the heel raise. Gastrocnemius is a biarticular muscle affecting, not only plantarflexion, but also knee flexion. Therefore, one could expect to see a bigger knee moment for leg presses than for squat as well, however one can not (see figure 24). This is probably because of the moments only representing the resultant of all muscle forces acting on the joint. Due to this, one could expect a higher activity for the FWED leg presses in the knee extensors to counteract the knee flexion created by gastrocnemius. However, no muscle activity from the squat has been analyzed in this pilot study and therefore no conclusion about this could be done. The small difference which could be seen between the moments of FWED1 and FWED0 can be explained by the segment mass of the shank and foot being influenced by gravitational force in FWED1.

The power of the squat being bigger than the FWED leg presses, seen in figure 24, was due to the higher knee angle velocity and the longer peak duration of the moment. Furthermore, the squat showed a power starting and returning to zero, this originates in the starting point and the ending point of the squat being static. In that case the muscles were working isometrically to keep the position, thus creating a net moment of zero. Oscillations were seen in the knee joint as well but not as much as in the ankle joint. The oscillations might have been caused by the altering load throughout the range of motion and the forced movement coming from the traction force produced

by the flywheel. When performing a squat the whole motion is controlled by the performer. Another explanation could be that the test subject was not very familiar with the device.

The major aspect that could be seen in the hip joint angles, shown in figure 25, was that the initial positions were totally different. In the squat, the test subject started from an upright standing position with the hip almost fully extended. In the flywheel leg press, the subject was siting down leaning slightly backwards, implicating a bigger hip flexion. The motion was also performed sitting with more or less the same inclination of the trunk, suggesting that the change of hip angle was caused by the flexion of the knee. The squat showed a quick hip flexion, induced by the wish to keep the balance through adjustment of the centre of gravity.

The difference in hip moment between FWED1 and FWED0 (see moment plot in figure 25) was caused by gravity. FWED1 showed a smaller moment because the weight of the trunk was contributing to the hip extension. In a zero gravity condition, however, the hip extension needed to be produced completely by the muscles themselves in order to counteract the traction force acting to flex the hip. It could also be seen that the squat created a similar, or slightly bigger, moment than FWED1 even though the reaction force of the leg press was higher. This can also be explained by the effect of the trunk assisting the hip in extension, in the squat gravity only contributed to flexion of the hip.

The power of squat was considerably bigger than the powers of FWED1 and FWED0, this can be seen in the hip power plot in figure 25. This was mainly because of, the same reasons as previously, the rapid change of angle and longer duration of moment peak. As the variation of hip angle in flywheel leg presses are reasonably small, small hip powers would also be expected.

Over all it was seen that the distribution of power in the different joints varied between the two exercises. In the flywheel leg presses the biggest powers were found in the ankle and the knee joints while in the squat it was found in the knee and the hip. However, it was difficult to draw conclusions from the power analysis due to the power being dependent on the net joint moment and the comparison between two different exercises. There were significant differences in terms of the motions being in different directions (along or perpendicular to the gravity vector), the loads being almost constant or changing and the ankles contributing to a heel raise or not. Furthermore, a profound disadvantage was the exercises being performed by two separate test subjects with different individual variances.

5.1.4 Simulated Activity

An expected result of ankle plantarflexor activity, see figure 26, would have been a higher activity in the soleus medialis muscle since soleus is the major contributor to plantarflexion. Instead, the results showed a high activity in both gastrocnemius muscles and some activity in soleus lateralis and no activity in soleus medialis in the middle of the exercise. This can be explained by how the simulation program solves the problem using the idea of effectiveness in the optimization part. The soleus lateralis produced enough force so that soleus medialis did not have to produce any force in order to drive the plantarflexion. The result showed that gastrocnemius was the muscle that used most of its capacity to drive the plantarflexion movement. Gastrocnemius is a biarticular muscle crossing both the ankle joint and the knee joint, but acts primarily as a plantarflexor. Even though most of the activation was induced to plantarflex, the activity did also contribute to flex the knee. To counteract this undesirable flexion of the knee, knee extensors were activated, and co-contraction of the knee was observed. This made sense, since there was a dip in the gastrocnemous activity and not in the soleus muscle. If the dip ascended in the ankle joint we would probably have seen a dip in the soleus muscle as well. This was confirmed by observing the activity of the knee extensors, see figure 27, where there was a dip at the same time point as for the gastrocnemius.

Furthermore, vastus lateralis was the muscle using most of its capacity, see figure 27, it is also known that vastus lateralis is the major knee extensor. Hence, it was the primary muscle driving the knee extension, as expected. Rectus femoris is a biarticular muscle acting both as a hip flexor and a knee extensor, but primary as a knee extensor. As rectus femoris did also flex the hip, see figure 30, hip extensors must also have been activated to counteract the hip flexion, i.e. there was co-contraction in the hip muscles.

There were no significant differences in the activity levels in the muscles between 1g and 0g conditions for ankle plantarflexors, see figure 26, and knee extensors, see figure 27. This could be explained by the segmental mass of the foot and shank being quite low. Hence, the external force was quite low compared to the produced muscle force, resulting in no notable differences between the two gravity conditions.

In contrast to ankle plantarflexors and knee extensors activity, there was a significant difference between the two gravity conditions in hip extensors, see figure 28. As explained in the previous paragraph, the external force depends on the segmental mass, this results in a distinguished difference between the two gravity conditions. The mass of the trunk was relatively high, and the gravity wanted to pull the trunk towards the ground, thus creating a

extension in the hip. While in the 0g environment the hip extensors had to create the same amount of force in order to keep the position, thus a higher activity could be seen among the hip extensor muscles in the 0g environment compared to the 1g environment.

It is known that the biceps femoris muscle is one of the primary hip extensors and the results showed most activity in the biceps femoris, see figure 28, which was expected. When a more vigorous extension was needed, the gluteus maximus was activated in order to contribute to the extension. Which could also be seen in the results in figure 28. Furthermore, gluteus maximus is the only unmitigated hip extensor. This could explain why the activity pattern in gluteus maximus deviated from the rest of the muscle patterns, as they also acted as knee flexors. There were also peaks in the beginning and end of the cycle. This was probably due to the recoil that occurred when the strap started to wind back, in the outer turning point. It was also known that the hip was affected by the trunk and associated muscles, which may cause activity and deviation in the activity pattern. This was not covered in this pilot study and more research is needed in order to explain the behavior of the hip.

As many of the hip extensors also act as knee flexors, extension of the hip may affect the knee flexion activity as well. The result from knee flexor activity, see figure 29, and hip extension activity, see figure 28, only differed by two muscles, which are the knee flexor, biceps femoris short head and the hip extensor, gluteus maximus. The activity of biceps femoris short head was almost non-existing through the whole cycle, however, small activations were indicated in the start and end of the cycle. The showed activity was probably not contributing to the movement and could therefore be neglected. As there was a traction force pulling the performer from the outer turning point towards the inner turning point, no force produced by the performer was required for this movement. The required force in order to perform the movement was added by the external traction force.

As already mentioned, gastrocnemius was activated to plantarflex the ankle, see figure 26. As gastrocnemius is a biarticular muscle, it would contribute to a knee flexion to some extent, hence, reducing the activity of the other knee flexor muscles.

As the traction force was attached to the trunk, it would force the hip to flex and therefore no internal force needed to be produced, hence, there was no activity in the hip flexors with the exception of rectus femoris, see figure 30. The activity of rectus femoris appeared because rectus femoris acted to extend the knee.

It was problematic to define how activity from biarticular muscles ap-

peared in the different joints. There were a lot of aspects to take into consideration when determining contribution to different joint movements. Attachment positions, attachment angles and lever arms were some of the aspects which need to be analyzed in order to determine the force and activity contribution to different joints. This was not covered in the pilot study and more research is needed to draw clear conclusions about muscle activity with respect to movement in different joints, although propositions can be obtained.

Overall, the activity was expected to be higher in all of the muscle groups. Since no EMG measurement was done during the FWED leg press it was challenging to confirm or deny the results of the activity level. However, as the same model was applied in the different simulations, conclusions regarding recruitment between the two gravity conditions were proposed. Furthermore, the recruitment of the muscles was reasonable, therefore conclusions regarding muscle recruitment between the two gravity conditions were proposed.

5.2 Laboratory Sessions

The squat and leg press exercises are considered to be largely 2-dimensional movements in this pilot study. Therefore, only flexion and extension for the three joints have been plotted. As some muscles have the ability to contribute to different joint movements, some activation may have been caused by movements in other directions than the ones covered in this report.

Since the results between Squat, FWED1 and FWED0 are compared, it would have been desirable to use same subjects for both exercise sessions. The results depend on the movement the subject performs. The ability to perform a movement depends a lot on physiological factors. These factors will affect the results, for example, muscle tissue compositions, strength and ability to perform a leg press and a squat. In order to draw clear conclusions from the comparison of a flywheel leg press and a squat, the subjects should have been the same. Using the same subject would increase the internal validity of the experiment. Another way to increase the internal validity is to do the exercise session in the same laboratory. The use of more test subjects would make the study more quantitative. Although no clear conclusions could be drawn from the comparison between a squat and flywheel leg press, due to mentioned reasons, indications could be identified and further research areas could be visualized from this pilot study. Nevertheless, using two different subjects was nothing that prevented from proposing conclusions from the comparison between FWED1 and FWED0.

A limitation in the experimental setup was the mounting of the force

plates on the frame of the used prototype of YoYo Multigym. The force plate was attached perpendicular to the gravity direction, while in the prototype the foot pad has an inclination in order to prevent heel raise. This was done in order to restrict the reaction force to the horizontal direction, since it is independent of gravity.

To increase the precision in the collected movements, more markers could have been used in the motion capture session. In the FWED leg press session 14 markers were used. Using more markers may have given a more accurate scaling of the model and of the simulated results. However, the used model was reliable for the purpose of this pilot study.

When experimental markers are placed on predetermined landmarks in order to be matched by AnyBody model markers, a type of soft tissue artifacts may distort, or cause error, in the scaling and the simulated movement. Soft tissue artifact in this context was when the skin was sliding upon the bone, for example when one puts a finger on the skin and starts to move the finger, the skin will then follow the finger movement but the bone will remain still.

One major simplification in the pilot study was the assumption of the traction force, and the negligence of the seat reaction force. During the laboratory session of the flywheel leg press, the traction force and seat reaction force were not measured, as no measurement devices were available. An assumption that the traction force would have the same amplitude, but in the opposite direction of the foot reaction force, was therefore done. When the performer pushed against the force plates with a certain amount of force, the approximated force pulled the performer via the strap. The seat reaction force was neglected, as this reaction force would not act in the same direction as the movement, thus not impact the movement significantly. It is also known that there was air resistance working on the system while performing a FWED leg press, but with no significant impact. Thus, the air resistance was neglected during the simulations.

The two different exercises, the squat and the FWED leg press, differed in the movement. It turned out that the experimental set up of the force plates on the FWED forced the subject to perform a heel raise in the inner and outer turning points. A more accurate comparison would be achieved if the FWED leg press was performed with an inclination of the force plates, avoiding a heel raise.

5.3 Modeling in AnyBody

The human body is a very complex system to model. Therefore a lot of simplifications and assumptions are made in order to make modeling possi-

ble. All these assumptions make it impossible to reproduce the functions of the human body completely and the results will differ from reality in some aspects.

The AnyBody Modeling System uses rigid body modeling, which means that the bones are modeled as rigid bodies, in reality the bones are flexible to some extent. Modeling bones as rigid bodies and not as flexible bodies will for example cause a longer lever arm, inducing a larger moment in the joints. Yet, this bone flexibility is very small and has a minimal contribution to changes of lever arms.

The joints are modeled as frictionless joints. In real joints there is some friction within the joints, caused by interaction between tissues. With a frictionless joint, a movement needs less force to be produced, i.e. the amount of force needed to produce the specific movement would be a bit higher in reality. Thus, it is slightly easier for a simulation model to produce a movement than for the real subject.

In modeling of the human body also the muscles are simplified in terms of being modeled as single elastic strings between two attachment points. In certain cases the strings have wrapping points or wrapping surfaces. The wrapping points and surfaces prevent the muscles from penetrating a bone or any other rigid body. Instead the string will then, via the wrapping point, take a pathway around the bone. However, the muscles modeled with wrapping will always be in contact with the wrapping points, even if the muscle in reality separates from the surface sometimes.

The used AnyBody model is based on studies by embalmed specimen and not the test subjects. Each human has an individual anatomical set up. Although anthropometry is statistically established data, studying a great selection of humans, everybody has an individual set up of body measurements. Thus, the model will diverge from the test subject in that aspect. The composition of different muscle fiber types is also varying between individuals and can affect the force generated. However the model uses the same composition for all test subjects.

The motion and parameter optimization study in AnyBody only takes body weight and marker placements into consideration while scaling the model. The composition of tissues as body fat and muscle mass is neglected in the tool procedure and therefore mass of body fat and muscle mass will be processed in the same way. Clearly, a larger amount of muscle mass will contribute more to muscle force capacity than the same weight of body fat will do. Therefore, the model of an obese subject can theoretically be the same as the model of a very muscular subject, if the marker positions are the same, although the capacity of producing force is clearly different between

them.

Moreover, the optimization process used by the software to decide the muscle forces is based on the assumption that the CNS aims for maximum synergism, i.e. the needed force is distributed on several muscles instead of letting one muscle do the whole work. However, the intention of the CNS is not commonly known and it is only an assumption.

In the modeling of the FWED leg press, the traction force was placed at a position differing from the real one for simplicity reasons. The point of action of the traction force was attached to the sternum instead of being somewhere in the abdomen area. This modification was considered to be justified in means of not jeopardizing the results in a significant way. However, we could expect to see a higher hip moment because of a longer lever arm, thus a higher activity in the hip extensors. Even though we got a deviation from the real internal hip moment the study was mainly to compare the leg press in 1g with the leg press in 0g. Since the same model was used in both cases the results from that point of view were not affected substantially.

Although the modeling of a human body implies many assumptions and simplifications, the deviations are considered to be insignificant. Using a biomechanical simulation software when accomplishing an analysis of a biomechanical system will give results very close to reality.

6 Recommendations for Future Work

At the end of this pilot study, new research areas were visualized and improvement actions were identified. These are presented below as recommendations of future work.

The same test subject should perform both exercises in order to achieve higher validity of the results. The experimental sessions should be performed in the same laboratory and the use of more test subjects are recommended to enable a quantitative analysis.

In order to confirm the activity level, EMG measurement during a leg press on a flywheel exercise device is recommended. To get a more accurate EMG measurement, intramuscular EMG is proposed.

The mounting of the force plates should be in the same angle as the footpad angle on the YoYo Multigym in order to avoid heel raise. If this is not possible, the squat should be performed with heel raise.

Measurement of all external forces, including foot reaction force, traction force and seat reaction force should be done to improve the accuracy of the simulation.

As the trunk has a great impact on the production of the movement, the trunk should be included in the analysis. Expanding the analysis to cover the motion in a third dimension will contribute to a better understanding of muscle actions.

It would be desirable to do additional simulations using a so called forward dynamic principle in order to get an idea of a potential difference in motion when performing a FWED leg press in microgravity.

The highest degree of accuracy would naturally be achieved by performing an exercise session in a microgravity environment, for example during a parabolic flight.

7 Conclusion

From this pilot study some conclusions are proposed, but more research is needed in order to draw general conclusions regarding effects of exercise on a flywheel exercise device in microgravity, compared to exercise on a flywheel exercise on earth and a body weighted squat on earth.

Performing a leg press on a flywheel exercise device on earth or in microgravity seems to provide as much or more joint moment in ankle, knee and hip compared to a body weighted squat performed on earth.

Performing a leg press on a flywheel exercise device in microgravity may generate a higher level of muscle activity among hip extensors and knee flexors compared to performing a leg press on a flywheel exercise device on earth.

References

[1] *NASA's Journey to Mars*, NASA, December 2014. [Online]. Available: http://www.nasa.gov/content/nasas-orion-flight-test-and-the-journey-to-mars/index.html#.VLADHlr82hZ

[2] J. C. B. Jr., *Space Physiology.* Oxford University Press Inc., 2006.

[3] (2014, August) Exercising in space. [Online]. Available: http://www.asc-csa.gc.ca/eng/astronauts/living-exercising.asp

[4] R. B. Setlow, "The hazards of space travel," *EMBO Reports*, vol. 4, no. 11, pp. 1013–1016, November 2003.

[5] (2015, January) Exercising in space. [Online]. Available: http://www.nasa.gov/centers/marshall/news/background/facts/astp.html

[6] (2014, July) Advanced resistive exercise device. [Online]. Available: http://www.nasa.gov/mission_pages/station/research/experiments/1001.html

[7] M. Pozzo, "The yoyo technology, fundaments and applications," June 2008, dept. of Physiology and Pharmacology, Karolinska Institutet, Stockholm, Sweden.

[8] A. Frechette, Private communication, November 2014, Wyle GmbH, Albin Koebis Strasse 4, Cologne, Germany.

[9] L. Norrbrand, M. Pozzo, and P. A. Tesch, "Flywheel resistance training calls for greater eccentric muscle activation than weight training," *European Journal of Applied Physiology*, vol. 110, no. 5, pp. 997–1005, November 2010.

[10] J. A. Cotter, A. Yu, F. Haddad, A. Kreitenberg, M. J. Baker, P. A. Tesch, K. M. Baldwin, V. J. Caiozzo, and G. R. Adams, "Concurrent exercise on a gravity-independent device during simulated microgravity," *Medicine and Science in Sports and Exercise*, July 2014, published ahead of Print.

[11] J. Hamill and K. M. Knutzen, *Biomechanical Basis of Human Movement*, 3rd ed. Philadelphia: Wolters Kluwer Health/Lippincott Williams and Wilkins, 2009.

[12] (2015, March) Nationalencyklopedin, osteoporos. [Online]. Available: http://www.ne.se/uppslagsverk/encyklopedi/l%C3%A5ng/osteoporos

[13] H. M. Frost, "Wolff's law and bone's structural adaptations to mechanical usage: an overview for clinicians," *The Angle Orthodontist*, vol. 64, no. 3, pp. 175–188, 1994.

[14] ——, "Bone's mechanostat: A 2003 update," *The Anatomical Record Part A*, vol. 275A, no. 2, pp. 1081–1101, 2003.

[15] H. Schiessl and J. Willnecker, *Muscle cross sectional area and bone cross sectional area in the lower leg measured with peripheral computed tomography in Musculoskeletal interactions.* Hylonome Editions, 1999, vol. II.

[16] H. M. Frost, "The utah paradigm of skeletal physiology: an overview of its insights for bone, cartilage and collagenous tissue organs," *Journal of Bone and Mineral Metabolism*, vol. 18, no. 6, pp. 305–316, 2000.

[17] O. College, Ed., *Anatomy & Physiology.* Rice University, April 2013. [Online]. Available: http://cnx.org/content/col11496/1.6/

[18] (2015, January). [Online]. Available: http://web.archive.org/web/20110718163549/http://anatomy.med.umich.edu/modules/joints_module/joints_02.html

[19] H. Gray, *Anatomy of the Human Body*, 20th ed., W. H. Lewis, Ed. Philadelphia: Lea & Febiger, 1918. [Online]. Available: http://www.bartleby.com/br/107.html

[20] D. G. Sale, "Neural adaption to resistance training," *Medicine and science in sports and exercise*, vol. 20, pp. 135–145, 1988.

[21] B. Lyndon. (2015, January) NASA. [Online]. Available: http://www.nasa.gov/pdf/64249main_ffs_factsheets_hbp_atrophy.pdf

[22] H. D. Young, R. A. Freedman, and A. L. Ford, *University Physics with modern physics*, 12th ed. Pearson International Edition, 2008.

[23] Everkinetic, *Illustration of a squat*, Wikimedia Commons, July 2010. [Online]. Available: http://commons.wikimedia.org/wiki/File:Squats.png?uselang=sv

[24] *YoYo Multigym*, YoYo Technology AB, Stockholm, Sweden. [Online]. Available: http://nhance.se/products/multigym/

[25] M. Damsgaard, J. Rasmussen, S. T. Christensen, E. Surma, and M. de Zee, "Analysis of musculoskeletal systems in the anybody modeling system," *Simulation Modelling Practice and Theory*, vol. 14, no. 8, pp. 1100 – 1111, 2006.

[26] (2014, December). [Online]. Available: http://www.clinicalgaitanalysis.com/teach-in/inverse-dynamics.html

[27] J. Beggs, *Kinematics*. Hemisphere Publishing Corporation, 1983.

[28] S. L. Delp, F. C. Anderson, A. S. Arnold, P. Loan, A. Habib, C. T. John, E. Guendelman, and D. G. Thelen, "Opensim: open-source software to create and analyze dynamic simulations of movement," *IEEE Transactions on Biomedical Engineering*, vol. 54, no. 11, pp. 1940–1950, November 2007.

[29] R. Stagni, S. Fantozzi, A. Cappello, and A. Cappozzo, "Advanced technologies for neuro-motor assessment and rehabilitation," in *Biomechanics of Human Movement*. Biomedical Engineering Unit, DEIS, University of Bologna and Department of Human Movement and Sport Sciences IUSM, Rome, 2006. [Online]. Available: http://www.starter-project.com/Presentazioni/Cappello.pdf

[30] W. Land, D. Volchenkov, B. E. Bläsing, and T. Schack, "From action representation to action execution: Exploring the links between cognitive and biomechanical levels of motor control," *Frontiers in Computational Neuroscience*, vol. 7, no. 127, p. 8, 2013.

[31] L. Sigal, "Marker-based motion capture," in *Human Motion Modeling and Analysis*, Sep 2012. [Online]. Available: http://www.cs.cmu.edu/~yaser/Lecture-3-MarkerBasedMocap.pdf

[32] (2014, June). [Online]. Available: http://www.organicmotion.com/motion-capture/

[33] *The AnyBody Modeling System*, AnyBody Technology A/S, Aalborg, Denmark. [Online]. Available: http://www.anybodytech.com

[34] M. D. Klein Horsman, H. F. J. M. Koopman, F. C. T. van der Helm, L. Poliacu Prose, and H. E. J. Veeger, "Morphological muscle and joint parameters for musculoskeletal modelling of the lower extremity," *Clinical Biomechanics*, vol. 22, no. 2, pp. 239 – 247, 2007.

[35] (2014, October). [Online]. Available: http://wiki.anyscript.org/index.php/AnyBody_Managed_Model_Repository:_Body_Models

[36] (2014, September). [Online]. Available: http://wiki.anyscript.org/index.php/NEW:_How_to_setup_your_own_MoCap_driven_Model

[37] A. Lindau. (2014, September) Gravity information system. [Online]. Available: http://www.ptb.de/cartoweb3/SISproject.php

Appendices

A Force Plate Attachment Parts

Figure 31: Upper attachment part.

Figure 32: Lower attachment part.

B Matlab Code of EMG Signal Processing

```
y=load('rectusfemoris.txt');
y2=detrend(y);
rect=abs(y2);
[a,b]=butter(5,10/1000,'low');
filter_y=filtfilt(a,b,rect);

plot(filter_y)
xlabel('Time [s]')
ylabel('EMG [10^-6 V],Äô)
```

C AnyBody Force Plate Class Template

```

#class_template ForcePlateType1 (PlateName, Folder,AnySeg &Limb, No, Fx, Fy, Fz, Px,Py,Mz ){

  #var AnySwitch Switch_DrawForceVectorFromCOP = On;

  AnyFixedRefFrame Corners ={
    AnyVar CoordinateSystemSize= 0.1;

    AnyRefNode c01={
      AnyInt i=0;
      AnyInt plnr=No;
      sRel=0.001*{Folder.Groups.FORCE_PLATFORM.CORNERS.Data[plnr][i][0],Folder.Groups.FORCE_PLATFORM.CORNERS.Data[No][i][1],Folder.Groups.FORCE_PLATFORM.CORNERS.Data[No][i][2]};
      AnyDrawNode drw={ScaleXYZ=0.01*{1,1,1};RGB={1,0,0};};
      AnyDrawVector  DrawName = {
        Vec = {0.0,0,0};  //use zero length
        Line.Thickness = 0.025; //arbitary value
        Text = "1"; //make reference to name
        Line.RGB={1,0,0};//make reference to color
      };
    };

    AnyRefNode c02={
      AnyInt i=1;
      AnyInt plnr=No;
      sRel=0.001*{Folder.Groups.FORCE_PLATFORM.CORNERS.Data[plnr][i][0],Folder.Groups.FORCE_PLATFORM.CORNERS.Data[No][i][1],Folder.Groups.FORCE_PLATFORM.CORNERS.Data[No][i][2]};
      AnyDrawNode drw={ScaleXYZ=0.01*{1,1,1};RGB={1,0,0};};
      AnyDrawVector  DrawName = {
        Vec = {0.0,0,0};  //use zero length
        Line.Thickness = 0.025; //arbitary value
        Text = "2"; //make reference to name
        Line.RGB={1,0,0};//make reference to color
      };
    };

    AnyRefNode c03={
      AnyInt i=2;
      AnyInt plnr=No;
      sRel=0.001*{Folder.Groups.FORCE_PLATFORM.CORNERS.Data[plnr][i][0],Folder.Groups.FORCE_PLATFORM.CORNERS.Data[No][i][1],Folder.Groups.FORCE_PLATFORM.CORNERS.Data[No][i][2]};
      AnyDrawNode drw={ScaleXYZ=0.01*{1,1,1};RGB={1,0,0};};
```

```
      AnyDrawVector  DrawName = {
        Vec = {0.0,0,0};  //use zero length
        Line.Thickness = 0.025; //arbitary value
        Text = "3"; //make reference to name
        Line.RGB={1,0,0};//make reference to color
      };
    };

    AnyRefNode c04={
      AnyInt i=3;
      AnyInt plnr=No;
      sRel=0.001*{Folder.Groups.FORCE_PLATFORM.CORNERS.Data[plnr][i][0],Folder.Groups.FORCE_PLATFORM.CORNERS.Data[No][i][1],Folder.Groups.FORCE_PLATFORM.CORNERS.Data[No][i][2]};
      AnyDrawNode drw={ScaleXYZ=0.01*{1,1,1};RGB={1,0,0};};
      AnyDrawVector  DrawName = {
        Vec = {0.0,0,0};  //use zero length
        Line.Thickness = 0.025; //arbitary value
        Text = "4"; //make reference to name
        Line.RGB={1,0,0};//make reference to color
      };

    };


    AnyRefNode PlateCenter={
      sRel=0.25*(.c01.sRel+.c02.sRel+.c03.sRel+.c04.sRel);
      AnyVec3 p1=sRel;
      AnyVec3 p2=0.5*(.c01.sRel+.c04.sRel);
      AnyVec3 p3=0.5*(.c01.sRel+.c02.sRel);
      ARel =RotMat(p1,p2,p3);

      //      AnyDrawRefFrame drw={ScaleXYZ=..CoordinateSystemSize*{1,1,1};RGB={0,1,0};};

    };

  };




  AnySeg ForcePlate={
    Mass=0.0;
    Jii={0,0,0};
    r0=.Corners.PlateCenter.sRel; // Initial position

```

```
85      //Rotational tranformation matrix for a coordinate system
        defined by three points. The first point is the origin of the
         system; the second gives the direction of the first (x) axis
        . Together all three points must span a plane which will be
        the plane of the first (x) and the second (y) axes, having
        the third (z) axis as normal.
86      AnyVec3 p1=.Corners.PlateCenter.sRel;
87      AnyVec3 p2=0.5*(.Corners.c01.sRel+.Corners.c04.sRel);
88      AnyVec3 p3=0.5*(.Corners.c01.sRel+.Corners.c02.sRel);
89      Axes0 =RotMat(p1,p2,p3);
90
91      AnyInt plnr=No;
92      AnyVar z_check = iffun(gtfun(Origins[plnr][2], 0), 1, -1);
93      AnyFloat Origins= Folder.Groups.FORCE_PLATFORM.ORIGIN.Data;
94      AnyMessage Origin_Z_value_message=
95      {
96        TriggerConst = iffun(gteqfun(.z_check,0), 1, 0);
97        Type = MSG_Message ;
98        Message = "The older AMTI origin has its Z value as
        positive. So this value is converted automatically. Please
        refer to www.c3d.org/HTML/type21.htm.";
99      };
100     //Transducer location
101     AnyRefNode TransducerLocation =
102     {
103       AnyFloat Origins= Folder.Groups.FORCE_PLATFORM.ORIGIN.Data
        ;
104       AnyVar xdist=.z_check*Origins[.plnr][0]*Folder.
        PointsScaleFactor;//distance from x axis on transducer to x
        axis of center of plate
105       AnyVar ydist=.z_check*Origins[.plnr][1]*Folder.
        PointsScaleFactor; //distance from y axis on transducer to y
        axis of center of plate
106       AnyVar zdist=.z_check*Origins[.plnr][2]*Folder.
        PointsScaleFactor;//distance from z axis on transducer to z
        surface of plate
107
108       sRel={xdist,ydist,zdist};
109       //AnyDrawRefFrame drw={ScaleXYZ=0.2*{1,1,1};RGB={1,0,0};};
         // Red coord system
110     };
111
112
113     AnyRefNode PlateGraphics ={
114       sRel={0,0,0.05};
115
116       AnyVec3 Size={vnorm(..Corners.c01.sRel-..Corners.c02.sRel
        ,2),vnorm(..Corners.c02.sRel-..Corners.c03.sRel,2),0.1};
117
```

```
      AnyDrawSurf DrwBox = {
        FileName = "box";
        RGB = 0.45*{1,1,1};
        ScaleXYZ=.Size/0.3;
        Opacity =0.4;
        Face=-1;
      };

    };


  };

  AnyKinEqSimpleDriver ForcePlateDriver ={
    AnyKinLinear ForcePlateLin={
      AnyRefNode &ref1=..Corners.PlateCenter;
      AnySeg &ref2=..ForcePlate;
      Ref=0;
    };

    AnyKinRotational ForcePlateRot={
      AnyRefNode &ref1=..Corners.PlateCenter;
      AnySeg &ref2=..ForcePlate;
      Type=RotAxesAngles;
    };
    DriverPos={0,0,0,0,0,0};
    DriverVel={0,0,0,0,0,0};
    //  Reaction.Type = {Off,Off,Off,Off,Off,Off};  //this plate is carried by global
  };

  //this is the new CoP segment
  AnySeg CoPSegment ={
    r0=.Corners.PlateCenter.sRel;
    Mass=0;
    Jii={0,0,0};
  //AnyDrawRefFrame drw={ScaleXYZ=0.2*{1,1,1};}; // Reference frame of GRF center, yellow
  };
  //linear measure between forceplate and Cop seg
  AnyKinLinear Lin ={
    Ref=0;
    AnyRefFrame &ref1=.ForcePlate.TransducerLocation ;
    AnySeg &ref2=.CoPSegment;
  };
  //Rotational  measure between forceplate and Cop seg
  AnyKinRotational Rot ={
    Type=RotAxesAngles;
    AnyRefFrame &ref1=.ForcePlate.TransducerLocation ;
```

```
    AnySeg &ref2=.CoPSegment;
  };
  //driver all dof except x and y to zero
  AnyKinEqSimpleDriver driver ={
    AnyKinLinear &ref1=.Lin;
    AnyKinRotational &ref2=.Rot;
    MeasureOrganizer={2,3,4,5};
    DriverPos={0,0,0,0};
    DriverVel={0,0,0,0};
    Reaction.Type={Off,Off,Off,Off};
  };
  //drive x and y position wrt to plate transducer location ?
  AnyKinEqInterPolDriver driveXY={
    Type=PiecewiseLinear;
    T=.Time;
    Data={Px,Py}*Folder.PointsScaleFactor;
    AnyKinLinear &ref=.Lin;
    MeasureOrganizer={0,1};
    Reaction.Type={Off,Off};   //reaction off
  };



  //create reactions between CoP seg and limb
    AnyReacForce PlateFootReaction={

    AnyKinLinear Lin={
      Ref=0;
       AnyRefFrame &ref1=..CoPSegment ;
      AnySeg &ref2=..Limb;
    };

    AnyKinRotational Rot={
      AnyRefFrame &ref1=..CoPSegment ;
      AnySeg &ref2=..Limb;
      Type=RotAxesAngles;
    };

  };



  AnyInt    EndFrame =Folder.Header.FirstFrameNo-1+(Folder.Header
    .LastFrameNo-Folder.Header.FirstFrameNo+1)* Folder.Header.
    NoAnalogSamplesPer3DFrame;
  AnyFloatVar   tStart = Folder.Header.FirstFrameNo/Folder.Header
    .VideoFrameRate;
  AnyFloatVar    tEnd =  Folder.Header.LastFrameNo/Folder.Header.
    VideoFrameRate;
```

```
210
211   AnyInt AnalogData=EndFrame-Folder.Header.FirstFrameNo;
212   AnyFloat Time=tStart+(iarr(0,AnalogData)*(tEnd-tStart)/
        AnalogData);
213
214
215   /// A lowpass butterworth filter
216   AnyFunButterworthFilter LowPassFilter =
217   {
218     FilterForwardBackwardOnOff = On;
219     AutomaticInitialConditionOnOff = On;
220     N = 2;
221     AnyVar CutOffFrequency=15;
222     AnyVar SampleFreq=Folder.Header.VideoFrameRate* Folder.
        Header.NoAnalogSamplesPer3DFrame    ;
223     W = {1/(SampleFreq*0.5)*CutOffFrequency};
224     Type = LowPass;
225   };
226
227
228
229   AnyFunInterpol load ={
230     Type=PiecewiseLinear;
231     T=.Time;
232     Data={Fx,Fy,Fz,Mz};
233     //   Data=.Cal'*{.LowPassFilter(Fx),.LowPassFilter(Fy),.
        LowPassFilter(Fz),.LowPassFilter(Mz)};
234
235   };
236
237
238   AnyVar FzTotal=load(ForcePlateDriver.t)[2];
239   AnyVar OnOff=iffun(gtfun(-FzTotal,10.0),1.0,0.0);
240
241   AnyForce3D Force ={
242
243     AnyRefFrame &ref=.CoPSegment ; // Force vector is shown in
        the CoP coord system
244     Flocal=.OnOff*{.load(.ForcePlateDriver.t)[0],.load(.
        ForcePlateDriver.t)[1],.load(.ForcePlateDriver.t)[2]};
245     AnyDrawVector DrawForce =      {
246       AnyRefFrame &ref=.ref;
247       Vec=.Flocal*1/1000;
248       PointAway = Off;  // Vector points "away"
249       DrawCoord = Off;
250
251       Line.RGB ={0,0,1};
252       Line.Thickness = 0.01;  // Showing the force
253       Line.End.Style = Line3DCapStyleArrow;
```

```
        Line.End.Thickness = 2*0.01;
        Line.End.Length = 4*0.01;
        GlobalCoord=Off;
      };


    };


    AnyMoment3D Moment ={

      AnyRefFrame  &ref=.ForcePlate.TransducerLocation ;
      Mlocal=.OnOff*{0,0,.load(.ForcePlateDriver.t)[3]}*Folder.PointsScaleFactor;
      AnyDrawVector DrawMoment =      {
        AnyRefFrame &ref=.ref;
        Vec=.Mlocal*1/1000;
        PointAway = Off;
        DrawCoord = Off;

        Line.RGB ={0,1,1};
        Line.Thickness = 0.01; // Turquoise plate in the upper left corner
        Line.End.Thickness = 2*0.01;
        Line.End.Length = 4*0.01;
        GlobalCoord=Off;
      };
    };

//  AnyFolder CenterOfPressure =
//  {
//    AnyForceMomentMeasure2 NetEffectMeasure =
//    {
//      AnyRefFrame& ref = ..ForcePlate;
//      AnyForceBase& Forces = ..Force;
//      AnyForceBase& Moments = ..Moment;
//
//      AnyVec3 Flocal = F*ref.Axes;
//      AnyVec3 Mlocal = M*ref.Axes;
//    };
//
//    AnyVar fx = NetEffectMeasure.Flocal[0];
//    AnyVar fy = NetEffectMeasure.Flocal[1];
//    AnyVar fz = NetEffectMeasure.Flocal[2];
//    AnyVar px = NetEffectMeasure.Mlocal[0];
//    AnyVar py = NetEffectMeasure.Mlocal[1];
//    AnyVar mz = NetEffectMeasure.Mlocal[2];
//
//    AnyVar fzz =iffun(gtfun(  (fz^2)^0.5,0),fz,fz+1000000);
```

```
//
//      AnyVar Vx= -py/fzz;
//      AnyVar Vy= px/fzz;
//      AnyVar Vz= 0;
//
//      AnyVar OnOff=.OnOff;
//
//      AnyRefFrame& ref_ForcePlate = .ForcePlate;
//      ref_ForcePlate  =
//      {
//        AnyDrawSphere COP_ball =
//        {
//          RGB = {0,1,0};
//          ScaleXYZ = 0.015 *{1,1,1};
//          //Opacity = iffun(gtfun(..fz, -10.0), 0.0, 1.0);
//          Opacity = ..OnOff;
//          Position = {..Vx, ..Vy, ..Vz};
//        };
//      };
//
//      AnyDrawLine Line =
//      {
//        p0 = {.Vx, .Vy, .Vz};
//        p1 = p0+0.004*.OnOff*{.fx, .fy, .fz};
//        Visible = ..Switch_DrawForceVectorFromCOP ;
//        AnyRefFrame &ref = ..ForcePlate;
//
//        Line.RGB ={0,0,1};
//        Line.Thickness = 0.01;
//        Line.End.Thickness = 2*0.01;
//        Line.End.Length = 4*0.01;
//        GlobalCoord=Off;
//      };
//
//   };

};
```

D Marker Positions for FWED Leg Press

Marker Name	Anatomical Position
HEAD	Top of the head
RACR	Right shoulder bone
LACR	Left shoulder bone
RASI	Right anterior superior iliac spine
LASI	Left anterior superior iliac spine
SACR	Sacrum
RKNE	Right lateral femur epicondyle
LKNE	Left lateral femur epicondyle
RHEE	Right calcaneus
LHEE	Left calcaneus
RTOE	2nd metatarsal head on right foot
LTOE	2nd metatarsal head on left foot
RANK	Right lateral malleolus
LANK	Left lateral malleolus

Table 1: Markers used during the laboratory session of the FWED leg press

E Marker Positions for Squat

Marker Name	Anatomical Position
LFHD	Left front head
RFHD	Right front head
LBHD	Left back head
RBHD	Right back head
C7	7th cervical vertebra
T10	10th thoracic vertebra
CLAV	In between the collar bones
STRN	Sternum
LACR	Left shoulder bone
RACR	Right shoulder bone
LASI	Left anterior superior iliac spine
RASI	Right anterior superior iliac spine
LPSI	Left posterior superior iliac spine
RPSI	Right posterior superior iliac spine
LTHI	Left thigh
RTHI	Right thigh
LKNE	Left lateral femur epicondyle
RKNE	Right lateral femur epicondyle
LTIB	Left shank
RTIB	Right shank
LHEE	Left calcaneus
RHEE	Right calcaneus
LTOE	2nd metatarsal head on left foot
RTOE	2nd metatarsal head on right foot
LANK	Left lateral malleolus
RANK	Right lateral malleolus

Table 2: Markers used during the laboratory session of the Squat

TRITA 2015:15